

High-temperature superconductivity: the current state

E G Maksimov

DOI: 10.1070/PU2000v043n10ABEH000770

Contents

1. Introduction and a few words about myths	965
2. What is a ‘conventional’ metal?	968
3. How far are superconducting cuprates from ‘conventional’ metals?	976
4. The enigma of the superconducting state in cuprates	982
5. Conclusion, or is there light at the end of the tunnel?	988
References	989

Abstract. Theoretical and experimental work concerning high-temperature superconductors in general and cuprates in particular is reviewed. A detailed analysis of the current knowledge of the subject suggests that when in the normal state, superconducting cuprates behave very much the same as ‘conventional’ metals. Experimental evidence is presented for the existence of strong relaxation processes in the normal state of HTSC systems at low energy. *Ab initio* calculations of the optical spectra and the electron–phonon interaction (EPI) show that the electron-phonon mechanism explains many features of low-energy relaxation processes in HTSC systems, including the high critical temperature. However, many properties of the superconducting state, for example, the anisotropic d pairing in cuprates, cannot be explained with the EPI mechanism alone. A number of models for cuprate superconductors with EPI and Coulomb repulsion are discussed in detail.

*Than vulgar truth we value higher
A flattering deception...*
A S Pushkin

1. Introduction and a few words about myths

The study of high-temperature superconductivity (HTSC) has been conducted for over 35 years. Two stages in its development can readily be distinguished which we may provisionally call ‘prehistoric’ and ‘historic’. The first stage began with the pioneering papers by Ginzburg [1] and Little [2] who hypothesized the existence of high-temperature superconductors due to the interaction of electrons not with phonons, but rather with electron excitations whose energy is much higher than the phonon energy. The beginning of the second stage can be associated with the publication by

Bednorz and Müller [3] who reported the probable observation of superconductivity in the compound $\text{La}_{2-x}\text{Ba}_x\text{CuO}_4$ with a record critical transition temperature $T_c \approx 30$ K.

Our definition of the two stages in the development of the HTSC problem is not evaluative, although these two stages are of course markedly distinct. The most serious of these distinctions is the scale of research and the number of publications. The number of papers on HTSC published after 1986 appreciably exceeds the total number of preceding publications on superconductivity beginning from its discovery in 1911. Furthermore, after the discovery of superconductivity in yttrium-containing cuprates (YBCO) [4] with $T_c \approx 90$ K and mercury-containing ones [5, 6] with $T_c \approx 135$ –160 K, the HTSC problem was no longer purely theoretical, but became practically significant owing to the possibility of exceedingly important technical applications. This fact was largely the cause of the inflow of money and researchers into this field. It was like a mudflow that almost completely washed out the memory of the rather fruitful stage of HTSC research prior to its experimental discovery.

The preliminary results of the first stage were summarized in book [7]. The basic achievements of this ‘prehistoric’ stage were as follows:

— the fact was clearly and definitely understood that along with the well-known electron–phonon mechanism of superconductivity due to electron–electron attraction through the phonon exchange, other mechanisms due to Coulomb interaction of electrons may also exist;

— the absence of strict limitations, at the level of the laws of nature, on the possible value of the critical temperature T_c of the superconducting transition was proved. The opposite hypothesis, which certainly had a negative effect on the development of HTSC research, was put forward by very competent experts in the theory of superconductivity — Anderson and Cohen [8];

— it was also proved that high T_c values can only be obtained in systems with strong local field effects, i.e., in systems with strong interaction [7, 9]. The point is not only that according to the well-known Bardeen – Cooper – Schrieffer (BCS) formula

$$T_c = 1.14\bar{\omega} \exp\left(-\frac{1}{\lambda}\right) \quad (1)$$

E G Maksimov P N Lebedev Physics Institute,
Russian Academy of Sciences
Leninskii prosp. 53, 117924 Moscow, Russian Federation
Tel. (7-095) 135-75 11. Fax (7-095) 135-85 33
E-mail: maksimov@lpi.ru

Received 10 May 2000
Uspekhi Fizicheskikh Nauk 170 (10) 1033–1061 (2000)
Translated by M V Tsaplina; edited by M V Magnitskaya

the temperature T_c is exponentially small for small coupling constants λ . The situation is somewhat more complicated. It was shown [7–9] that a necessary, but not sufficient condition for the existence of high T_c is the presence of negative values of the static dielectric function $\varepsilon(\mathbf{q}, 0) < 0$. This inequality may only hold, as was rigorously proved in [7, 9], in systems with strong interaction (see also the recent review [10]);

— various factors that determine the value of T_c for the phonon mechanism of superconductivity were thoroughly analyzed [11]. Further investigations of metal oxides, nitrides, and carbides, in which phonon frequencies may be high because of the low oxygen, nitrogen, and carbon atomic masses, were acknowledged as promising. The crucial role of ionicity in these compounds, which leads to a noticeable increase of the matrix element of the electron–phonon interaction (EPI), was revealed. In the metallic compounds well-known by that time, the atoms of the light elements unfortunately do not participate in EPI since their electronic states are deep under the Fermi surface.

Alongside the very fact of the experimental discovery of corresponding systems and the above-mentioned scales of research, the new stage in the development of the HTSC problem had some other distinctions, including those in theoretical approaches. As has already been mentioned, it became clear rather long ago that high T_c values may only exist in systems with strong interaction. At the ‘prehistoric’ stage, a concrete study of such HTSC systems was not given sufficient attention. The second-stage research was, on the contrary, largely devoted to the investigation of the effects of strong exchange-correlation interaction and their manifestations in both the normal and superconducting states.

Most of the theoretical work exploited the Hubbard model whose crucial point is strong Coulomb repulsion of electrons at one site. Two most radical ideas concerning the nature of high-temperature superconductivity in cuprates were suggested in precisely the framework of the Hubbard model [12, 13]. These ideas were based on the so-called resonant valence bond model [14] describing the spin liquid of singlet electron pairs and, in fact, amply rested on the results obtained for one-dimensional models of interacting electrons. In the latter models, the low-temperature behavior of electrons differs drastically from the standard behavior in ordinary three-dimensional systems. An electron possessing charge and spin stops being a well defined excitation. The so-called charge-spin separation occurs. The spin is transported by an uncharged fermion, typically called a spinon, and the charge — by a spinless excitation called a holon. As distinct from an ordinary Fermi liquid, such a system is usually referred to as a Luttinger liquid [15]. The basic idea, due to Anderson [12], concerning the nature of HTSC systems is that the electron system in such compounds is precisely a Luttinger liquid in both the normal and superconducting states.

The author of the present review does not dare describe the details of this approach because they have been modified rather radically over the past decade. A seriously revised version was presented by Anderson in 1999 [16].

The idea suggested by Laughlin et al. [13] differs from Anderson’s approach in the use of fractional statistics for the description of low-energy excitations in HTSC systems. This means that the corresponding excitations are neither bosons nor fermions. In quantum field theory they are termed ‘anyons’. It is important that the anyon theory leads to a violation of time-reversal symmetry because spontaneous

magnetic fluxes actually appear in the system. To all appearances, the experimental data [17, 18] reject such a possibility. The majority of researchers are not enthusiastic about the HTSC theory developed by Anderson either [19] (see also the critical review [20] of book [12]).

A great many theoretical studies of HTSC compounds have been reduced at the second, as well as the first stage to a rather standard procedure. A system of quasi-particle electronic excitations is considered, but instead of phonons and excitons, which lead to electron–electron attraction and pairing, something different is introduced. These may be spin fluctuations [21, 22], the formation of ‘spin bags’ [23, 24], a specific band structure possessing a so-called ‘nesting’ [25], etc.

The only distinction of the second stage is a more comprehensive investigation of models based on strong electron–electron repulsion which may cause an anisotropic d-pairing. The very possibility of the appearance of a superconducting state in systems with interparticle repulsion is not at all new. It was first formulated by Kohn and Luttinger [26] who showed that the electron pairing in such systems may occur not in an isotropic s-channel, but in higher harmonics. The possibility of pairing due to the interaction with spin fluctuations was also pointed out rather long ago by Akhiezer and Pomeranchuk [27]. By the time HTSC was discovered in cuprates, p-pairing in liquid ^3He [28], again due to spin fluctuations, as well as possible d-pairing in heavy fermion systems [29] was already known. Attempts are still made to construct anisotropic models of HTSC systems using various mechanisms of electron–electron attraction (see surveys [30, 31]). We shall return to the discussion of these questions in sections to follow, but before that we would like to speak a little about the numerous myths circulating around the HTSC problem from its appearance to the present date.

One of the first myths was initiated by the talk of the distinguished American physicist-experimenter, Matthias, at the first HTSC conference in 1966 when he compared this problem with a UFO. Thus, the HTSC problem itself was treated by many researchers as a myth. And this was the only one of all the myths which, although having done much harm to the search for HTSC materials, evaporated after 1986. The others turned out to be much more tenacious. One of them was mentioned at the beginning of this section. This was the statement by Cohen and Anderson [8] claiming the existence of a very strong limitation upon the possible increase of T_c values due to electronic mechanisms of attraction owing to the inequality

$$\varepsilon(\mathbf{q}, 0) > 0, \quad (2)$$

which, according to the authors of [8], is the criterion of system stability. Kirzhnits showed [32] that the stability condition for a system of charged particles actually comes down to the inequality

$$\frac{1}{\varepsilon(\mathbf{q}, 0)} < 1, \quad (3)$$

which holds for both $\varepsilon(\mathbf{q}, 0) > 1$ and $\varepsilon(\mathbf{q}, 0) < 0$. Moreover, it was demonstrated [33] that owing to the phonon contribution to $\varepsilon(\mathbf{q}, 0)$ the existence of negative $\varepsilon(\mathbf{q}, 0)$ values is not only possible, but even inevitable for many stable systems, in particular, for many metals. As an aside, we note that for a wide range of momenta \mathbf{q} , negative $\varepsilon(\mathbf{q}, 0)$ values exist [33, 34]

in a well-known system (which, however, is not directly related to HTSC), namely, in molten common salt. Nevertheless, the assertion that the inequality $\varepsilon(\mathbf{q}, 0) < 0$ cannot be valid is still roaming about the literature, the same as the suggestion, also expressed in paper [8], that within the phonon mechanism of superconductivity T_c cannot exceed 40 K.

The second stage of HTSC studies brought about sundry new myths. One of them can be presented in the form of a table which persistently emerges in many surveys, original papers, and invited talks at international HTSC conferences. A fragment of this table is reproduced in Fig. 1. Discussions of this table customarily involve additional declarations of the type: “The most vivid proof of the unusual behavior of HTSC systems is the linear temperature dependence of their electrical resistivity.” What can be said about this? First of all, there is not a single so-called ‘conventional’ metal in nature with resistivity proportional to T^2 over a reasonably wide temperature range. One can readily make sure of this by looking at Fig. 2 which was taken from the famous manual by Kittel [35]. It illustrates the temperature dependence of electrical resistivity ρ described by the standard Bloch–Grüneisen formula allowing for EPI effects. This formula can be written in the form

$$\rho = A \left(\frac{T}{\Theta_D} \right)^5 \int_0^{\Theta_D/T} \frac{x^5 dx}{\sinh^2 x}, \quad (4)$$

where A is the material constant of a metal and Θ_D is the kinetic Debye temperature which may differ from the corresponding thermodynamic quantity. Figure 2 shows that at temperatures $T \geq \Theta_D/5$ the metal resistivity behaves, according to the Bloch–Grüneisen formula, as

$$\rho \sim T. \quad (5)$$

Thus, the resistivity of the majority of metals depends linearly on T even at temperatures $T \sim 40\text{--}100$ K. Consequently, the linear dependence $\rho(T)$ observed in superconducting cuprates at $T \sim 40\text{--}80$ K cannot be thought of as something essentially different from all other — ‘conventional’ — metals. We shall discuss this question in more detail below, and now we shall only note that, as can be seen from Fig. 2, the universal dependence $\rho(T)$ is demonstrated not solely by simple metals (Al), but by transition and even magnetic ones (Ni) as well.

Another myth (or more precisely, a whole mythology) is associated with the Landau Fermi-liquid theory. Most papers, both theoretical and experimental, devoted to HTSC cuprates state something like this: “There is not the slightest doubt that the electron system in these compounds exhibits non-Fermi-liquid behavior”. To gain insight into this problem, we shall formulate the basic idea of the Landau

Metal	Conventional	High T_c
Resistivity	$\rho \sim T^2$	$\rho \sim T$
Quasiparticle lifetime, $1/\tau(T, \omega)$	$aT^2 + b\omega^2$	$aT + b\omega$
Spin excitation spectrum	Flat	Peaked at $\mathbf{Q}_i \sim (\pi/a, \pi/a)$

Figure 1. Typical understanding of differences between HTSC systems and other metals.

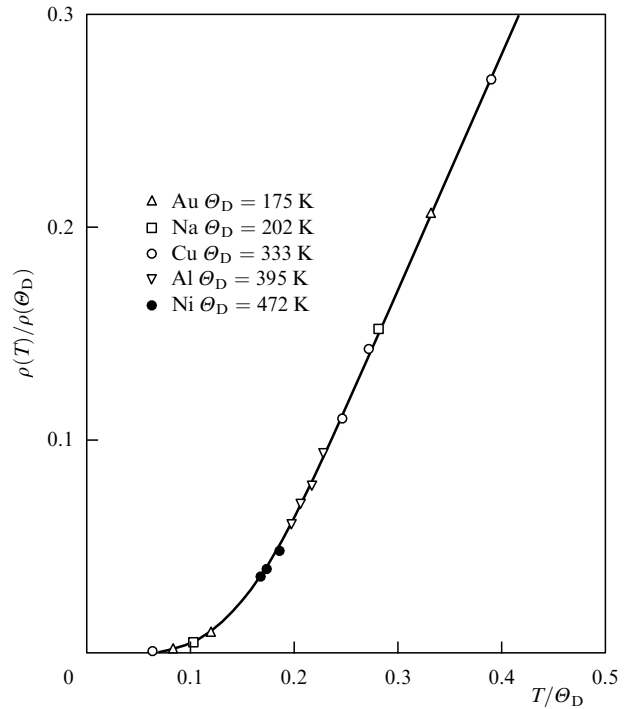


Figure 2. Temperature dependence of electrical resistivity. The solid curve is plotted according to the Bloch–Grüneisen formula. Experimental points for some metals are presented.

Fermi-liquid theory: “A system of strongly interacting Fermi particles at sufficiently low temperatures $T < T^*$ and energies $\omega < \omega^*$ behaves like a Fermi gas of weakly interacting quasi-particles having a well defined Fermi surface and the quasi-particle damping $1/\tau \sim \omega^2$. The volume of the Fermi surface for quasi-particles is the exactly same as that for non-interacting particles, and each quasi-particle possesses a charge $\pm e$ and a spin $\pm 1/2$ ”.

A large number of papers appeared devoted to the calculation (for some models) of temperatures T^* and energies ω^* describing the crossover, as termed by the authors, from the ‘Fermi-liquid’ to the ‘non-Fermi-liquid’ behavior. In the first place, all these statements contain at least a linguistic mistake: the quantities T^* and ω^* describe the crossover not from the ‘Fermi-liquid’ to the ‘non-Fermi-liquid’ behavior, but from the Fermi-gas and universal behavior ($1/\tau \sim \omega^2$, $\rho \sim T^2$) to the non-universal, namely, Fermi-liquid behavior. Apart from the linguistic confusion, another thing is important: the quantities T^* and ω^* themselves, as well as the behavior of the system for $T > T^*$ and $\omega > \omega^*$, are specific properties of each particular model, and detailed investigation of them contributes little to the general insight into the physics of Fermi systems.

Several models exist in which the Landau Fermi-liquid theory is indeed violated. This means that even as $T \rightarrow 0$ and $\omega \rightarrow 0$, the fermion system is not described by the model of a quasi-particle gas with a certain charge and spin. We have already given such an example — the Luttinger liquid — which describes a one-dimensional electron gas. Other models also exist (see the recent review [36]). This problem is fairly interesting in itself and deserves serious research, but another thing is of importance, too. The point is that the Landau Fermi-liquid theory can in fact be literally applied to none of the ‘conventional’ or ‘unconventional’ metals. Not a single

metal exists in which relaxation is due to the weak interaction of quasi-particles, as it should be according to the Landau theory. Relaxation in metals is caused by EPI, by the interaction of electrons with collective excitations (spin or charge fluctuations), or by some more complicated processes. This can be readily understood from the particularly simple estimates of the relaxation rate obtained by Allen [37]. At high enough temperatures

$$\Theta_D < T \ll \varepsilon_F, \quad (6)$$

where ε_F is the Fermi energy of an electron, the expression for the inverse time of relaxation due to EPI, $1/\tau_{\text{epb}}$, and to the electron–electron interaction, $1/\tau_C$, can be written as

$$\frac{1}{\tau_{\text{epb}}} = 2\pi N(0) |\langle V_{\text{epb}} \rangle|^2 \left[\frac{2T}{\Theta_D} \right], \quad (7)$$

$$\frac{1}{\tau_C} = 2\pi |\langle V_C \rangle|^2 [N(0)T]^2. \quad (8)$$

Here $N(0)$ is the density of electron states on the Fermi surface, V_{epb} is the EPI matrix element, and V_C is the matrix element of the electron–electron Coulomb interaction. The quantities

$$\lambda_{\text{epb}} = \frac{N(0) |\langle V_{\text{epb}} \rangle|^2}{\Theta_D} \quad \text{and} \quad \lambda_C = N(0) |\langle V_C \rangle|^2 \quad (9)$$

are respectively the electron–phonon and the Coulomb interaction constants. Normally, $\lambda_{\text{epb}} \approx \lambda_C \approx 1$. The quantities $[2T/\Theta_D]$ and $[N(0)T]^2$ may be interpreted as the numbers of, respectively, phonons and electron-hole pairs. At temperatures corresponding to the inequality (6), the number of phonons is several orders of magnitude greater than the number of electron-hole pairs. As a result, the inverse time of relaxation due to EPI is several orders of magnitude greater than that due to the residual Coulomb quasi-particle interaction. The situation may change only at very low temperatures, when the EPI-induced relaxation decreases strongly as $1/\tau_{\text{epb}} \sim T^5$.

As is seen already from this section, this review may hardly claim completeness and impartiality in what concerns the presentation of the current state of HTSC problem and the discussion of most of the relevant papers. First, it is impossible not only to read all the publications available, but even to get acquainted with all the books on this subject. Second, the time of impartial and perfectly objective surveys of this problem has not yet come because, as P Anderson said, “the only consensus here is an absolute lack of consensus”. Nevertheless, the author assures the reader that he will not juggle with the facts nor ‘sweep the dust under the rug’ although he is naturally not going to conceal his own opinion about most of the questions touched upon in the review.

2. What is a ‘conventional’ metal?

The skepticism expressed in the preceding section in respect of a whole number of works on the Fermi liquid theory, which were carried out in the framework of HTSC research, not in the least concerns L D Landau or his extremely fruitful theory of quasi-particles [38]. Rather long ago, from the first papers by Bloch on the quantum theory of solids [39], electrons in metals were noticed to behave like non-interacting or weakly

interacting particles. But in actuality, no weak interaction exists in metals. One can easily make sure of this by taking the simplest model of metal, the so-called homogeneous electron gas. The energy per electron in such a system can be written as [40]

$$E = \frac{2.2099}{r_s^2} - \frac{0.9163}{r_s} - 0.096 + 0.0622 \ln r_s. \quad (10)$$

Here r_s is a dimensionless parameter related to the electron density n as

$$\frac{4\pi}{3} (r_s a_B)^3 = \frac{1}{n}, \quad (11)$$

where a_B is the Bohr radius of the electron.

The first term in formula (10) describes the contribution of the kinetic energy, the second — the contribution of the exchange energy and the last two — the contribution of the correlation energy. When there exists a weak interaction between particles in the system, the contribution of the kinetic energy substantially exceeds all the other contributions due to interparticle interaction. As can be seen from (10), in a homogeneous electron gas this situation is realized only for $r_s < 1$. In real metals, the mean density of conduction electrons is such that r_s for them lies in the interval $2 \leq r_s \leq 6$. Thus, even from the point of view of the homogeneous gas model, electrons in all metals represent a system of strongly interacting particles. Moreover, the model of a homogeneous electron gas is hardly suitable for the description of the properties of transition metals, where the d-electron density is rather far from homogeneous. This circumstance may in fact only enhance the exchange-correlation effects compared to the homogeneous electron gas model. In this connection L D Landau used to say: “Nobody has abrogated the Coulomb law”.

The Fermi liquid theory, first created by Landau for uncharged particles, was extended to the case of metals [41] and then fruitfully employed [42] to describe many low-temperature phenomena in metals. As was mentioned in the introduction, the relaxation processes in metals, at least at not very low temperatures, are not at all described by a weak residual interaction of quasi-particles. Furthermore, as is seen for instance from Fig. 2, in the majority of metals they are caused by EPI. This statement is valid not only for non-magnetic, but for most magnetic metals as well. Their electrical resistivity is also normally described by the Bloch–Grüneisen formula, and it is only for sufficiently high temperatures $T \geq 300\text{--}400$ K that the dependence $\rho(T)$ may become nonlinear obviously owing to the interaction among electrons and spin waves. The scale of these deviations from linearity is much smaller than the $\rho(T)$ values themselves. This means that the electron–spin wave interaction itself is markedly smaller than EPI.

The idea of the description of the relaxation processes in the Landau theory is extremely simple and consists in the construction of a quasi-classical Boltzmann equation. Suppose we somehow managed to find the energy of quasi-particle excitations $\varepsilon(\mathbf{k}, \mathbf{r}, t)$ for any point \mathbf{r} and its velocity $\mathbf{v}_\mathbf{k} = \partial\varepsilon/\partial\mathbf{k}$. Then, with $\varepsilon(\mathbf{k}, \mathbf{r})$ as the system Hamiltonian, the Boltzmann equation for the one-particle distribution function $f(\mathbf{k}, \mathbf{r}, t)$ of quasi-particles can be written as

$$\frac{\partial f}{\partial t} + \left(\frac{\partial f}{\partial \mathbf{r}} \frac{\partial \varepsilon}{\partial \mathbf{k}} - \frac{\partial f}{\partial \mathbf{k}} \frac{\partial \varepsilon}{\partial \mathbf{r}} \right) + F_{\text{ext}} \frac{\partial f}{\partial \mathbf{k}} = I(f). \quad (12)$$

Here F_{ext} is the external force acting on quasi-particles and $I(f)$ is the collision integral.

In the framework of the standard Landau theory, $\varepsilon(\mathbf{k}, \mathbf{r}, t)$ has the form

$$\varepsilon(\mathbf{k}, \mathbf{r}, t) = \varepsilon_0(\mathbf{k}) + \sum_{\mathbf{k}'} f(\mathbf{k}, \mathbf{k}') \delta f(\mathbf{k}', \mathbf{r}), \quad (13)$$

where $f(\mathbf{k}, \mathbf{k}')$ is the Landau interaction function.

The substitution of this expression into (12) yields a closed expression for the kinetic equation, the collision integral $I(f)$ being commonly neglected. This approach is easily extended to the allowance for the electron–phonon interaction. To this end, the dependence of $\varepsilon(\mathbf{k}, \mathbf{r}, t)$ on ion coordinates $\{\mathbf{R}_n\}$ should be added to (13). After that the function $\varepsilon(\mathbf{k}, \mathbf{r}, t, \{\mathbf{R}_n\})$ can be expanded in small ion displacements \mathbf{u}_n from equilibrium positions \mathbf{R}_n^0 :

$$\varepsilon(\mathbf{k}, \mathbf{r}, t, \{\mathbf{R}_n\}) = \varepsilon(\mathbf{k}, \mathbf{r}, t) + \sum_n \frac{\delta \varepsilon}{\delta \mathbf{R}_n} \mathbf{u}_n. \quad (14)$$

Writing then the equations for the displacements \mathbf{u}_n and expanding them in phonon variables, one can completely solve the problem of relaxation in a system of weakly interacting electron quasi-particles. The criterion of applicability of this approach is precisely the presence of well defined quasi-particles, that is, the validity of the inequality

$$\varepsilon_0(\mathbf{k}) \gg \frac{1}{\tau}. \quad (15)$$

Here $1/\tau$ is the relaxation rate and the energy $\varepsilon(\mathbf{k})$ is counted from the chemical potential. As we shall see in what follows, criterion (15) holds for metals only at very low temperatures, if at all. Already at $T \gtrsim \Theta_D/5$ EPI alone is enough for electrons to stop being well defined quasi-particles, and criterion (15) is certainly violated.

Nevertheless, the approach developed by Landau can also be extended to the Fermi liquid behavior of the system [37, 43–45] with a much softer condition than (15), namely

$$\frac{1}{\tau} \ll \varepsilon_F, \quad (16)$$

where ε_F is the Fermi energy of electrons. As a result, one can obtain a generalized Boltzmann equation using the technique of the many-body theory and Green functions and either the analytical continuation of the functions from imaginary frequencies [44] or the Keldysh technique [45] for time Green functions. A more extensive consideration of these questions goes far beyond the scope of the present review. We shall only note here that the EPI calculation in this approach comes down to the solution of a many-body problem with the Fröhlich Hamiltonian

$$H = H_e + H_{\text{ph}} + H_{\text{eph}}. \quad (17)$$

Here H_e describes the quasi-stationary electron state in a rigid lattice

$$H_e = \sum_{\mathbf{k}, \lambda} \varepsilon_{\mathbf{k}\lambda} c_{\mathbf{k}\lambda}^\dagger c_{\mathbf{k}\lambda}, \quad (18)$$

where $\varepsilon_{\mathbf{k}\lambda}$ is the energy of electron states in the λ band. H_{ph} is the Hamiltonian of non-interacting phonons

$$H_{\text{ph}} = \sum_{\mathbf{q}, \nu} \omega_{\mathbf{q}\nu} \left(b_{\mathbf{q}\nu}^\dagger b_{\mathbf{q}\nu} + \frac{1}{2} \right), \quad (19)$$

$\omega_{\mathbf{q}\nu}$ being the energy of phonon with polarization ν . H_{eph} is the EPI Hamiltonian

$$H_{\text{eph}} = \sum_{\mathbf{k}, \mathbf{q}, \nu, \lambda, \lambda'} g_{\mathbf{k}+\mathbf{q}, \mathbf{k}}^{(\nu, \lambda, \lambda')} c_{\mathbf{k}+\mathbf{q}, \lambda}^\dagger c_{\mathbf{k}, \lambda'} (b_{-\mathbf{q}\nu}^\dagger + b_{\mathbf{q}\nu}), \quad (20)$$

where $g_{\mathbf{k}', \mathbf{k}}^{(\nu, \lambda, \lambda')}$ is the EPI matrix element. In the framework of this approach kept in the spirit of the Landau Fermi-liquid theory, all the above defined quantities, such as $\varepsilon_{\mathbf{k}\lambda}$, $\omega_{\mathbf{q}\nu}$, and $g_{\mathbf{k}', \mathbf{k}}^{(\nu, \lambda, \lambda')}$ are some phenomenological parameters with values obtainable only from comparison with experimental data.

The above approach is in fact based on the assumption that electrons in a rigid lattice that undergo Coulomb interaction among themselves and with ions are well described by the Landau Fermi-liquid theory, i.e., they are well defined quasi-particles for which criterion (15) holds and the corresponding temperatures T^* and energies ω^* of the crossover from the Fermi-gas to the Fermi-liquid behavior are sufficiently large. Such metals to a first approximation will be thought of as ‘conventional’, although even such metals may demonstrate what seems at first glance a rather odd, so-to-say, ‘marginal’ behavior due to precisely the electron–phonon interaction. In a more general context, ‘conventional’ metals are those for which criterion (16) holds. These in particular may be metals exhibiting low-frequency spin and charge density collective excitations. As will be shown below, for metals possessing no such excitations and having T^* and ω^* largely exceeding the characteristic phonon energies Θ_D , many properties can in fact be completely calculated from the so-called ‘first principles’ [46] using the density functional theory (DFT).

Studies of the Fröhlich Hamiltonian have a long history, and the related problems may be considered as solved in many respects. The properties of the normal metal state described by this Hamiltonian were first investigated by Migdal [47] and the properties of the superconducting state by Eliashberg [48]. The kinetic properties of this model were also analyzed [45, 49]. We shall not dwell at length here on the derivation of the various formulas for the systems described by the Fröhlich Hamiltonian because a large number of books and reviews have been devoted to this subject (see, e.g., reviews [50, 51] and the references therein). We shall still present some formulas which are necessary for us here but restrict ourselves to only a few explanatory notes.

In order to describe the one-particle properties of the Fröhlich Hamiltonian, it is required that the electron and phonon Green functions be calculated. They can be written in the form

$$G^{-1}(\mathbf{k}, \lambda, \omega) = G_0^{-1}(\mathbf{k}, \lambda, \omega) - \Sigma(\mathbf{k}, \lambda, \omega) \quad (21)$$

and

$$D^{-1}(\mathbf{q}, \nu, \omega) = D_0^{-1}(\mathbf{q}, \nu, \omega) - \Pi(\mathbf{q}, \nu, \omega). \quad (22)$$

Here $G_0(\mathbf{k}, \lambda, \omega)$ is the Green function of noninteracting electrons which is defined by the Hamiltonian H_e (18) and $D_0(\mathbf{q}, \nu, \omega)$ is the Green function of phonons for the Hamiltonian (19)

$$D_0(\mathbf{q}, \nu, \omega) = \frac{2\omega_{\mathbf{q}\nu}}{\omega^2 - \omega_{\mathbf{q}\nu}^2 + i\delta}. \quad (23)$$

We shall first of all note [51] that in the framework of the approach considered here, the renormalization of the Green

function of phonons due to the electron – phonon interaction would be a double allowance for EPI because all the effects of adiabatic interaction of electrons with ion displacements should have already been taken into account in the definition of the phonon frequencies $\omega_{\mathbf{q}\nu}$. The Fröhlich Hamiltonian can only be exploited to calculate nonadiabatic effects in the phonon spectra. This means that when determining $D(\mathbf{q}, \nu, \omega)$, one should use the quantity $\Pi(\mathbf{q}, \nu, \omega) - \Pi(\mathbf{q}, \nu, 0)$ instead of the polarization operator $\Pi(\mathbf{q}, \nu, \omega)$. For the greater part of the phonon spectrum this quantity is small in the order of smallness of the ratio $\omega_{\mathbf{q}\nu}/\varepsilon_F$ and can therefore be neglected.

As was first shown by Migdal [47], the Green function $G(\mathbf{k}, \lambda, \omega)$ can be calculated exactly because in the Dyson equation for this function the high-order corrections can be neglected since $\bar{\omega}/\varepsilon_F$ ($\bar{\omega}$ is the mean phonon frequency) is small. The self-energy part $\Sigma(\mathbf{k}, \lambda, \omega)$ of the Green function can be written as

$$\Sigma(\mathbf{k}, \lambda, \omega) = \frac{1}{\pi N(0)} \int d\Omega \sum_{\mathbf{k}', \lambda', \nu} \left| g_{\mathbf{k}, \mathbf{k}'}^{(\nu, \lambda, \lambda')} \right|^2 \delta(\varepsilon_{\mathbf{k}', \lambda'}) \times \text{Im} D(\mathbf{k}' - \mathbf{k}, \nu, \Omega) L(\omega, \Omega), \quad (24)$$

the function $\Sigma(\mathbf{k}, \lambda, \omega)$ depending only on the position of the vector \mathbf{k}_F on the Fermi surface. As we noted earlier, the phonon Green function $D(\mathbf{q}, \nu, \Omega)$ need not be renormalized within this approach, and therefore

$$\text{Im} D(\mathbf{q}, \nu, \Omega) = \pi \delta(\omega_{\mathbf{q}\nu} - \Omega). \quad (25)$$

The function $L(\omega, \Omega)$ has the form

$$L(\omega, \Omega) = -2\pi i \left[n(\Omega) + \frac{1}{2} \right] + \Psi \left(\frac{1}{2} + i \frac{\Omega - \omega}{2\pi T} \right) - \Psi \left(\frac{1}{2} - i \frac{\Omega + \omega}{2\pi T} \right), \quad (26)$$

where $\Psi(x)$ is the digamma-function and $n(\Omega)$ is the Bose function. Introducing the EPI spectral density $\alpha_{\mathbf{k}}^2(\Omega)F(\Omega)$ equal to

$$\alpha_{\mathbf{k}}^2(\Omega)F(\Omega) = \frac{1}{N(0)} \sum_{\mathbf{k}', \lambda', \nu} \left| g_{\mathbf{k}, \mathbf{k}'}^{(\nu, \lambda, \lambda')} \right|^2 \delta(\omega_{\mathbf{k}' - \mathbf{k}, \nu} - \Omega) \delta(\varepsilon_{\mathbf{k}', \lambda'}), \quad (27)$$

one can rewrite the expression for $\Sigma(\mathbf{k}, \lambda, \omega)$ in the standard form

$$\Sigma(\mathbf{k}, \lambda, \omega) = \frac{1}{\pi} \int_0^\infty d\Omega \alpha_{\mathbf{k}}^2(\Omega) F(\Omega) L(\omega, \Omega). \quad (28)$$

The function $\Sigma(\omega)$, which yields the average value of the self-energy part

$$\Sigma(\omega) = \frac{1}{N(0)} \sum_{\mathbf{k}, \lambda} \delta(\varepsilon_{\mathbf{k}\lambda}) \Sigma(\mathbf{k}, \lambda, \omega) \quad (29)$$

can be defined as

$$\Sigma(\omega) = \int d\Omega \alpha^2(\Omega) F(\Omega) L(\omega, \Omega). \quad (30)$$

The function $\alpha^2(\Omega)F(\Omega)$ introduced above is customarily called the EPI spectral density or the Eliashberg function

and has the form

$$\alpha^2(\Omega)F(\Omega) = \frac{1}{N(0)} \sum_{\mathbf{k}, \lambda, \mathbf{k}', \lambda'} \left| g_{\mathbf{k}, \mathbf{k}'}^{(\lambda, \lambda', \nu)} \right|^2 \delta(\Omega - \omega_{\mathbf{k}' - \mathbf{k}, \nu}) \times \delta(\varepsilon_{\mathbf{k}\lambda}) \delta(\varepsilon_{\mathbf{k}'\lambda'}). \quad (31)$$

This function also defines, in particular, the superconducting properties of metals.

The self-energy part has real and imaginary parts and can be represented as

$$\Sigma(\omega) = -\omega \lambda(\omega, T) - \frac{i}{2\tau(\omega, T)}. \quad (32)$$

It is a well-known fact that the function $\lambda(\omega, T)$ characterizes the EPI-induced electron mass renormalization:

$$\frac{m^*(\omega, T)}{m} = 1 + \lambda(\omega, T), \quad (33)$$

and the function $\tau(\omega, T)$ describes the electron lifetime. The electron Green function has the form

$$G(\mathbf{k}, \omega) = \left[\frac{m^*(\omega, T)}{m} \omega - \varepsilon_{\mathbf{k}} + \frac{i}{2\tau(\omega, T)} \right]^{-1}. \quad (34)$$

The EPI-induced electrical conductivity $\sigma(\omega)$ of metals can be calculated using the Fröhlich Hamiltonian. We shall not present the related calculations [37, 49, 52, 53], but shall write $\sigma(\omega)$ in a form rather closely resembling the expression for the one-particle Green function:

$$\sigma(\omega) = \frac{\omega_{\text{pl}}^2}{4\pi} \left[-i\omega \frac{m_{\text{tr}}(\omega, T)}{m} + \frac{1}{\tau_{\text{tr}}(\omega, T)} \right]^{-1}. \quad (35)$$

The expression for the transport mass renormalization $m_{\text{tr}}(\omega, T)/m$ and the transport relaxation rate (or the inverse lifetime) $1/\tau_{\text{tr}}(\omega)$ has the form [37, 52, 53]

$$\omega \frac{m_{\text{tr}}(\omega, T)}{m} + \frac{i}{\tau_{\text{tr}}(\omega, T)} = \omega + 2 \int_0^\infty d\Omega \alpha_{\text{tr}}^2(\Omega) F(\Omega) \times K \left(\frac{\omega}{2\pi T}, \frac{\Omega}{2\pi T} \right), \quad (36)$$

where

$$K(x, y) = \frac{i}{y} + \left\{ \frac{y-x}{x} \left[\Psi(1 - ix + iy) - \Psi(1 + iy) \right] \right\} - \{y \rightarrow -y\}. \quad (37)$$

In the description of transport processes and, in particular, optical conductivity $\sigma(\omega)$, there occurs one more EPI spectral density $\alpha_{\text{tr}}^2(\Omega)F(\Omega)$ which has the form [36, 52, 53]

$$\alpha_{\text{tr}}^2(\Omega)F(\Omega) = \frac{1}{N(0) \langle v_F^2 \rangle} \sum_{\mathbf{k}, \mathbf{q}} \left| g_{\mathbf{k}, \mathbf{k}+\mathbf{q}}^{(\lambda, \lambda', \nu)} \right|^2 v_F (v_{F\lambda} - v'_{F\lambda'}) \times \delta(\varepsilon_{\mathbf{k}\lambda}) \delta(\varepsilon_{\mathbf{k}+\mathbf{q}, \lambda'}) \delta(\Omega - \omega_{\mathbf{q}\nu}). \quad (38)$$

Here v_F is the electron velocity on the Fermi surface and $\langle v_F^2 \rangle$ is the mean square velocity on the Fermi surface

$$\langle v_F^2 \rangle = \frac{1}{N(0)} \sum_{\mathbf{k}, \lambda} v_F^2 \delta(\varepsilon_{\mathbf{k}\lambda}). \quad (39)$$

This quantity is directly related to the plasma energy ω_{pl} included in the definition of optical conductivity (35):

$$\omega_{\text{pl}}^2 = \frac{4\pi e^2 N(0)}{3} \langle v_{\text{F}}^2 \rangle. \quad (40)$$

To make the picture more complete, we shall present the Eliashberg equations determining the superconducting properties of strong EPI systems. These equations involve two functions, namely, the order parameter $\Delta(\omega)$ and the renormalization function $Z(\omega)$. In the normal state, the quantity $\Delta(\omega)$ is naturally equal to zero and the renormalization function is related to the self-energy part $\Sigma(\omega)$ introduced above as

$$Z(\omega) = 1 - \frac{\Sigma(\omega)}{\omega}. \quad (41)$$

The Eliashberg equations themselves have the form

$$\begin{aligned} Z(\omega)\Delta(\omega) &= \int_{-\infty}^{+\infty} d\omega' \operatorname{Re} \left[\frac{\Delta(\omega')}{\sqrt{\omega'^2 - \Delta^2(\omega')}} \right] \\ &\times \int_0^{\infty} d\Omega \alpha^2(\Omega) F(\Omega) \left[\frac{f(-\omega') + n(\Omega)}{\omega' + \Omega - \omega} \right. \\ &+ \left. \frac{f(\omega') + n(\Omega)}{\omega' - \Omega - \omega} \right] - \mu(\varepsilon_{\text{F}}) \\ &\times \int_0^{\varepsilon_{\text{F}}} d\omega' \operatorname{Re} \left[\frac{\Delta(\omega')}{\sqrt{\omega'^2 - \Delta^2(\omega')}} \right] \tanh \frac{\omega'}{2T}, \quad (42) \end{aligned}$$

$$\begin{aligned} [1 - Z(\omega)]\omega &= \int_0^{\infty} d\omega' \operatorname{Re} \left[\frac{\omega'}{\sqrt{\omega'^2 - \Delta^2(\omega')}} \right] \\ &\times \int_0^{\infty} d\Omega \alpha^2(\Omega) F(\Omega) \left[\frac{f(-\omega') + n(\Omega)}{\omega' + \Omega + \omega} \right. \\ &- \frac{f(-\omega') + n(\Omega)}{\omega' + \Omega - \omega} + \frac{f(\omega') + n(\Omega)}{-\omega' + \Omega + \omega} \\ &- \left. \frac{f(\omega') + n(\Omega)}{-\omega' + \Omega - \omega} \right]. \quad (43) \end{aligned}$$

Here $f(\omega)$ is the Fermi function and $\mu(\varepsilon_{\text{F}})$ is the averaged Coulomb interaction.

As can be seen from the above consideration, the physical properties of a strong EPI system are defined by a set of various EPI spectral densities. To describe the optical spectra and the superconducting properties of quasi-isotropic metals, two such functions suffice, namely, the Eliashberg function $\alpha^2(\Omega)F(\Omega)$ and the transport spectral function $\alpha_{\text{tr}}^2(\Omega)F(\Omega)$. To consider the other kinetic properties, such as the Hall effect or the thermal electromotive force, other spectral densities may be needed as well. A large number of EPI spectral densities also occur in the analysis of systems with a strongly anisotropic EPI. The above results can be extended to this case using the expansion of all the functions under study in a certain complete and orthogonal basis possessing the crystal symmetry. As such a basis one can choose, for instance, the Fermi-harmonics basis set introduced by Allen [50].

In the framework of the standard Landau Fermi-liquid theory [38], the effects of quasi-particle interaction are described with the help of several phenomenological constants — angular harmonics of the Landau interaction

function $f(\mathbf{k}, \mathbf{k}')$ whose exact values can be found from comparison of theoretical results with experimental data. The Fermi-liquid description of strong EPI systems leads to the appearance of EPI spectral densities, i.e., not separate parameters, but functions which are also quite undefined within the Fermi-liquid approach itself. Fortunately, such functions can also be found in this case from comparison of theory with experiment. We shall return to the discussion of this question later, and now we shall consider several important, but not very well known results concerning the behavior of relaxation rates $1/\tau$ in strong EPI systems. Employing expression (34) for the one-particle Green function, we can write the expression for the quasi-particle energy in the form

$$E_{\mathbf{k}} = \frac{m}{m^*(\varepsilon_{\mathbf{k}}, T)} \varepsilon_{\mathbf{k}} - \frac{i}{2\tau^*(\varepsilon_{\mathbf{k}}, T)}, \quad (44)$$

where

$$\frac{1}{\tau^*(\varepsilon_{\mathbf{k}}, T)} = \frac{m}{m^*(\varepsilon_{\mathbf{k}}, T)} \frac{1}{\tau(\varepsilon_{\mathbf{k}}, T)}. \quad (45)$$

Well defined quasi-particles naturally exist under the condition

$$\frac{1}{2\tau^*(\varepsilon_{\mathbf{k}}, T)} \ll E_{\mathbf{k}}. \quad (46)$$

Considering that the quantity $1/\tau^*(0, T)$ at $T > \Theta_{\text{D}}/5$ can be written in the form

$$\frac{1}{\tau^*(0, T)} = 2\pi\lambda T, \quad (47)$$

where λ is the electron–phonon coupling constant

$$\lambda = 2 \int_0^{\infty} \frac{d\Omega}{\Omega} \alpha^2(\Omega) F(\Omega), \quad (48)$$

as well as the fact that as $\omega \rightarrow \infty$ we have

$$\frac{1}{\tau^*(\infty, T)} = \pi\lambda \langle \omega \rangle, \quad (49)$$

where

$$\lambda \langle \omega \rangle = 2 \int_0^{\infty} d\Omega \alpha^2(\Omega) F(\Omega) \coth \frac{\Omega}{2T}, \quad (50)$$

we can readily make sure that for most metals the condition of quasi-particle description (46) is violated over a vast temperature T and energy ω range.

Another important circumstance, which is given little attention too, is the appreciable difference between the one-particle $1/\tau^*(\omega, T)$ and transport $1/\tau_{\text{tr}}^*(\omega, T)$ effective inverse relaxation times. Figure 3 shows the behavior of these quantities as functions of ω for several temperature values for lead as calculated in our paper [51]. We shall discuss the principles of such calculations in what follows, and now we would only like to pay attention to the distinctions between these quantities. As is well-known [52], the one-particle relaxation rate reaches its maximum at an energy of the order of the maximum phonon frequency ω_{max} and then

stops being energy-dependent. In contrast with this, the transport relaxation rate is seen from Fig. 3 to continue increasing up to $\omega \sim 10\omega_{\max}$. In the case of high-temperature superconductors we have $10\omega_{\max} \approx 1$ eV, and therefore the assertions, very often encountered in the literature, that EPI is in principle incapable of explaining the relaxation processes measured in optical experiments and based on the assumption that $1/\tau_{\text{tr}}^*(\omega, T) = \text{const}$ for $\omega > \omega_{\max}$ are obviously groundless.

The last point to emphasize is the universal character of the energy and temperature dependences of the transport relaxation time. Figure 4, taken from our paper [53], shows the dependence of $1/\tau_{\text{tr}}^*$ on ω/ω_{\max} for six different situations. This means that six curves are actually plotted in the graph, which however all coincide in dimensionless variables. The transport coupling constant is expressed by a formula analogous to (48) but with the function $\alpha^2(\Omega)F(\Omega)$ replaced by $\alpha_{\text{tr}}^2(\Omega)F(\Omega)$. Thus, the energy dependence of the relaxation time is universal, while the absolute values are mainly determined by two quantities: the electron–phonon cou-

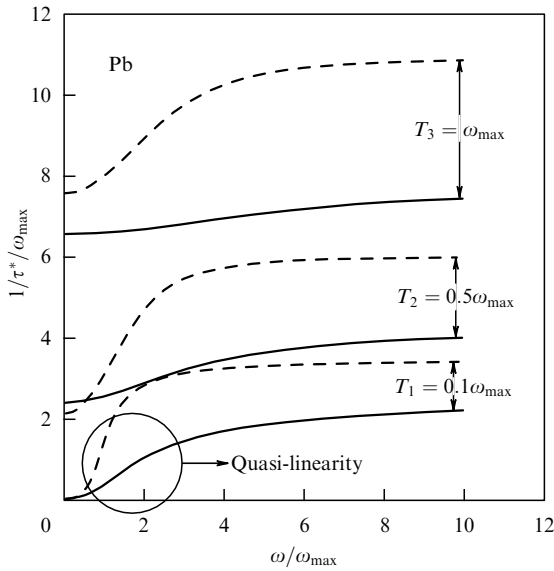


Figure 3. Comparison of the one-particle $1/\tau^*(\omega)$ (dashed lines) and the transport $1/\tau_{\text{tr}}^*(\omega)$ (solid lines) relaxation rates. The energy and the quantities $1/\tau^*(\omega)$ and $1/\tau_{\text{tr}}^*(\omega)$ are measured in units of $\omega_{\max} = 100$.

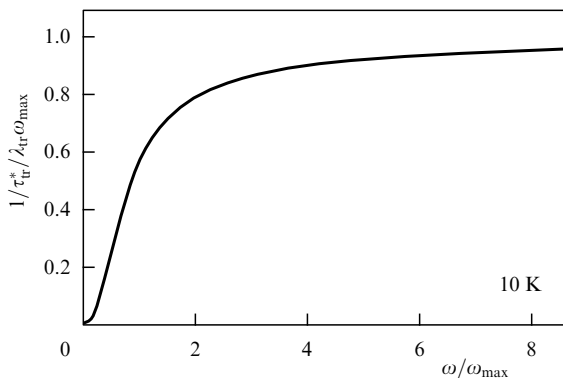


Figure 4. Transport relaxation rate $1/\tau_{\text{tr}}^*(\omega)$ at $T = 10$ K for different coupling constants $\lambda_{\text{tr}} = 0.2, 0.6, 1.0, 1.4$ and different phonon spectra with $\omega_{\max} = 612 \text{ cm}^{-1}, 735 \text{ cm}^{-1}, 882 \text{ cm}^{-1}$.

pling constant λ and the maximum phonon frequency ω_{\max} . In this respect, as will be seen in the section to follow, high-temperature superconductors are actually (quantitatively) different from many other metals. The matter is that in cuprates ω_{\max} assumes values of the order of 0.1 eV and the coupling constant λ may reach values of ~ 2 .

Does this universality of the transport relaxation time imply that all the other properties of metals with strong EPI are also universal? Of course not. So, for example, the Hall coefficient, which in many metals has a weak temperature dependence, in such a conventional metal as Al changes by more than an order of magnitude from helium to room temperatures [37]. In copper it demonstrates a rather strong and nonmonotonic temperature dependence. A very strong temperature dependence of the Hall coefficient is observed, for example, in TiC, ZrC, and VC carbides [54] although none of these metals is superconducting. The behavior of the thermal electromotive force of metals is even less universal. The lack of universality in the behavior of metals is especially obvious at low temperatures. In particular, in a number of quite conventional metals, such as copper, the one-particle relaxation rate is very anisotropic [55], and to explain this fact one should consider more general spectral densities than the averaged Eliashberg function $\alpha^2(\Omega)F(\Omega)$.

We shall now briefly discuss the above-mentioned possibility of obtaining EPI spectral densities from the analysis of experimental data. Such a possibility for the Eliashberg function $\alpha^2(\Omega)F(\Omega)$ was revealed rather long ago by McMillan and Rowell [56]. The work was based on processing experimental data on the behavior of the tunnel current at the superconductor–insulator–normal metal (SIN) transition. At low temperatures, the junction conductivity, i.e. the quantity $\partial I(V)/\partial V$, is expressed in this case in terms of the density of electron states in a superconductor:

$$\frac{\partial I}{\partial \omega} = N(\omega) = \text{Re} \left[\frac{\omega}{\sqrt{\omega^2 - \Delta^2(\omega)}} \right], \quad (51)$$

where $\omega = eV$.

McMillan and Rowell showed that knowing the value of $N(\omega)$ from experiment, one can solve the inverse problem for the Eliashberg equations and determine the function $\alpha^2(\omega)F(\omega)$. Such a procedure was performed for a large number of conventional superconductors and the function $\alpha^2(\omega)F(\omega)$ was obtained. This function appeared to look much the same in form as the density of phonon states $F(\omega)$, where

$$F(\omega) = \sum_{\mathbf{q}, \nu} \delta(\omega - \omega_{\mathbf{q}\nu}). \quad (52)$$

This was largely the reason why the Eliashberg function was written in the form of the product of a certain function $\alpha^2(\omega)$ by $F(\omega)$, although in actuality this is simply a unified function of energy ω defined by relation (31). Figure 5 presents a fragment of the function $N(\omega)$ for Pb. One can clearly see the nonmonotonic behavior of the function $N(\omega)$ for $\omega > \Delta$, where the magnitude of the superconducting gap Δ corresponds to the peak on the curve $N(\omega)$. It is in fact from this nonmonotonic dependence $N(\omega)$ that, as was shown by the physicists of Donetsk (Ukraine) [57], the information on the Eliashberg function is obtained. Furthermore, one can have an idea of the form of the function $\alpha^2(\omega)F(\omega)$ also without solving the inverse problem because the function $\partial^2 I(V)/\partial V^2$

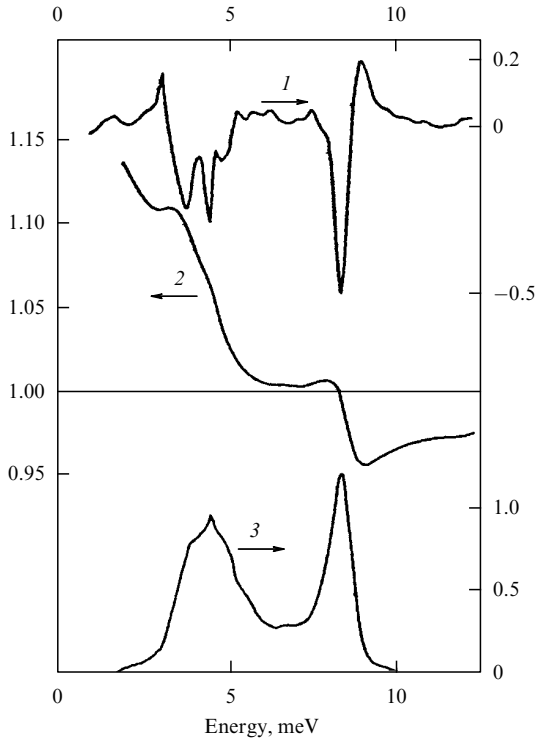


Figure 5. 1 — Derivative of the density of states with respect to energy, $\partial^2 I / \partial V^2$; 2 — the density of states of superconducting Pb; 3 — the quantity $\alpha^2(\omega)F(\omega)$ found by inversion of the Eliashberg equation for the gap $\Delta(\omega)$.

in the nonmonotonic domain reproduces the form of $\alpha^2(\omega)F(\omega)$ with the only difference being that the maxima of the function $\alpha^2(\omega)F(\omega)$ correspond to the minima of the function $\partial^2 I(V) / \partial V^2$ and vice versa.

Allen [52] suggested a procedure for obtaining the transport spectral density $\alpha_{tr}^2(\omega)F(\omega)$ from measurements of the optical conductivity $\sigma(\omega)$. This can most easily be done for $T \ll \Theta_D$. Expression (36) for the relaxation rate can in this case be written as [52, 53]

$$\frac{1}{\tau_{tr}(\omega)} = \frac{2}{\omega} \int_0^\omega d\Omega (\omega - \Omega) \alpha_{tr}^2(\Omega) F(\Omega), \quad (53)$$

wherefore it is readily seen that

$$\frac{d^2}{d\omega^2} \left(\omega \frac{1}{\tau_{tr}(\omega)} \right) = 2\alpha_{tr}^2(\omega)F(\omega). \quad (54)$$

And according to formula (35), $\omega[1/\tau_{tr}(\omega)]$ can be represented in the form

$$\omega \frac{1}{\tau_{tr}(\omega)} = \frac{\omega_{pl}^2}{4\pi} \omega \operatorname{Re} \left[\frac{1}{\sigma(\omega)} \right]. \quad (55)$$

Thus, expressions (54) and (55) completely solve the problem of finding the function $\alpha_{tr}^2(\omega)F(\omega)$ from experimental data on the optical spectra of metals at low temperatures $T \ll \Theta_D$. However, there are actually no papers reporting the application of this procedure to conventional metals for finding the function $\alpha_{tr}^2(\omega)F(\omega)$. The complexity of such studies is largely due to the important role of anomalous skin-effect in such metals [58], which is the cause of the difficulties in determining the optical conductivity $\sigma(\omega)$ for sufficiently small ω

corresponding to the region of the phonon spectra. Nonetheless, the corresponding studies were carried out for superconducting lead [59] where the light absorption coefficient was measured. The simplified expression, due to Allen [52], for the optical conductivity $\sigma_s(\omega)$

$$\sigma_s(\omega) = \frac{\omega_{pl}^2}{4\pi\omega} \frac{1}{\omega\tau_{tr}^s}, \quad (56)$$

where

$$\frac{1}{\tau_{tr}^s(\omega)} = \frac{2}{\omega} \int_0^{\omega-2\Delta} d\Omega (\omega - \Omega) E \left\{ \left[1 - \frac{4\Delta^2}{(\omega - \Omega)^2} \right]^{1/2} \right\} \times \alpha_{tr}^2(\Omega) F(\Omega). \quad (57)$$

was used for the relaxation rate in the superconducting state. In this expression, $E(x)$ is a total elliptic integral of second kind. Formulas (56) and (57) were obtained under much simplifying assumptions allowing for the electron scattering by phonons but neglecting the dependence of the order parameter Δ on the energy ω . A somewhat detailed analysis of the validity of the corresponding approximations has not yet been carried out.

The possibility of obtaining the function $\alpha_{tr}^2(\omega)F(\omega)$ for the superconducting state by direct differentiation of $\omega[1/\tau_{tr}^s(\omega)]$ by analogy with formula (54) has not been examined either.

The inverse problem was solved in paper [59], where the known $1/\tau_{tr}^s(\omega)$ was used to calculate the function $\alpha_{tr}^2(\Omega)F(\Omega)$ from expression (57). The results of processing show that the function $\alpha_{tr}^2(\omega)F(\omega)$ coincides rather well with the Eliashberg function obtained from the analysis of tunneling data, although the transport function possesses a much more pronounced structure. This may perhaps be explained by the special role of some phonon modes in the electron scattering by phonons. Some papers have recently appeared devoted to the determination of the transport spectral density also for high-temperature superconductors, but we shall discuss this point more extensively in the next section of the review.

As has already been mentioned, the knowledge of only two EPI spectral densities, i.e. the functions $\alpha^2(\Omega)F(\Omega)$ and $\alpha_{tr}^2(\Omega)F(\Omega)$, does not of course allow the description of all the thermodynamic and kinetic properties of metals especially if these metals show substantial anisotropy of either the Fermi surface or the electron-phonon scattering. The dream of many researchers in the field of solid state theory was therefore the creation of a procedure allowing *ab initio* calculations of the electron and phonon spectra of metals and the matrix elements of the electron-phonon interaction. Such attempts [60] were made long ago within the so-called electronic band-structure theory. A rather comprehensive discussion of this problem can be found in our reviews [51, 61], and now we shall very briefly consider the basic principles of such calculations and present some concrete results obtained in this way.

The *ab initio* electronic band theory is based on the method of the density functional [62] proposed by Kohn. Applying this method, one can reduce the calculation of the ground-state properties (as well as the thermodynamic functions) of a system of electrons interacting with one another and with the external potential (the nuclear potential in the case of crystals) to the solution of one-particle problem for the electron in a self-consistent field.

The corresponding Schrödinger equation (called the Kohn–Sham equation) has the form [62]

$$\left[-\frac{1}{2m}\nabla^2 + \sum_n V_n(\mathbf{r} - \mathbf{R}_n) + e^2 \int \frac{n(\mathbf{r}') d\mathbf{r}'}{|\mathbf{r} - \mathbf{r}'|} + V_{xc}(\mathbf{r}) \right] \times \psi_{\mathbf{k}\lambda}(\mathbf{r}) = \varepsilon_{\mathbf{k}\lambda} \psi_{\mathbf{k}\lambda}(\mathbf{r}), \quad (58)$$

and the electron density is expressed in a standard way in terms of the wave functions $\psi_{\mathbf{k}\lambda}(\mathbf{r})$:

$$n(\mathbf{r}) = \sum_{\mathbf{k}, \lambda}^{\varepsilon_{\mathbf{k}\lambda} = \mu} |\psi_{\mathbf{k}\lambda}(\mathbf{r})|^2, \quad (59)$$

where μ is the chemical potential. The condition

$$\varepsilon_{\mathbf{k}\lambda} = \mu \quad (60)$$

specifies the corresponding Fermi surface in the case of metals. The quantity $V_{xc}(\mathbf{r})$ is the so-called exchange-correlation potential

$$V_{xc}(\mathbf{r}) = \frac{\delta E_{xc}\{n(\mathbf{r})\}}{\delta n(\mathbf{r})}, \quad (61)$$

where $E_{xc}\{n(\mathbf{r})\}$ is the exchange-correlation energy functional dependent on the electron density. The exact value of this functional is unknown, and in calculations the local density approximation is typically used:

$$E_{xc}\{n(\mathbf{r})\} = \int \varepsilon_{xc}[n(\mathbf{r})] n(\mathbf{r}) d\mathbf{r},$$

where the function $\varepsilon_{xc}[n(\mathbf{r})]$ is replaced by its value for a homogeneous electron gas of the same density n . Solutions of equation (58), determined within DFT, describe the electronic band structure of a crystal.

In the first place we shall point out the similarity of the Kohn–Sham equation to Landau’s quasi-particle problem for a system of interacting electrons in a rigid lattice discussed earlier. Equation (58) also describes a set of electronic states in a rigid lattice, but formally they have no more similarities. The electron energies $\varepsilon_{\mathbf{k}\lambda}$ obtained from the Kohn–Sham equation in the framework of DFT formally have no physical meaning. Moreover, the Fermi surface determined by these energies from condition (60) is not obliged to coincide with the measured one [63] either. Furthermore, with allowance for the nonlocality of exchange-correlation effects these two surfaces must not coincide [64]. The point is that a real Fermi surface in a metal, as was shown by Luttinger [65], is described by an equation quite different from (58), namely,

$$\left[-\frac{\nabla^2}{2m} + \sum_n V_n(\mathbf{r} - \mathbf{R}_n) + e^2 \int \frac{n(\mathbf{r}') d\mathbf{r}'}{|\mathbf{r} - \mathbf{r}'|} \right] \psi_{\mathbf{k}\lambda}(\mathbf{r}) + \int d\mathbf{r}' \Sigma_{xc}(\mathbf{r}, \mathbf{r}', 0) \psi_{\mathbf{k}\lambda}(\mathbf{r}') = \varepsilon_{\mathbf{k}\lambda} \psi_{\mathbf{k}\lambda}(\mathbf{r}). \quad (62)$$

Here $\Sigma_{xc}(\mathbf{r}, \mathbf{r}', 0)$ is the exchange-correlation self-energy part of the exact one-particle Green function. Equation (62) may be regarded as a definition of another electronic band structure of a crystal.

Even mathematically, equations (58) and (62) differ notably from each other because the exchange-correlation potential $V_{xc}(\mathbf{r})$ is a local operator and $\Sigma_{xc}(\mathbf{r}, \mathbf{r}', 0)$ is a nonlocal integral operator, and the eigenvalues of these

equations, i.e. the quantities $\varepsilon_{\mathbf{k}\lambda}$, cannot be coincident in the general case. Unfortunately, it is rather difficult to find out how much these quantities actually differ since the electronic band structure corresponding to equation (62) has never been calculated for real metallic systems. A single paper [66] apparently exists presenting numerical calculations of the band structure from equation (62) for a one-dimensional Hubbard chain and showing that the given band structure possesses a whole number of rather specific properties.

It should immediately be noted that the band structure obtained either from (62) or (58) does not describe the spectrum of one-particle excitations of the system of electrons in a metal. This spectrum is determined by the one-particle Green function $G(\mathbf{r}, \mathbf{r}', \omega)$ which has the form

$$G^{-1}(\mathbf{r}, \mathbf{r}', \omega) = -\frac{\nabla^2}{2m} + \sum_n V_n(\mathbf{r} - \mathbf{R}_n) + e^2 \int \frac{n(\mathbf{r}') d\mathbf{r}'}{|\mathbf{r} - \mathbf{r}'|} - \Sigma_{xc}(\mathbf{r}, \mathbf{r}', \omega). \quad (63)$$

As is seen from this formula, the spectrum of one-particle excitations is specified not only by the nonlocal coordinate dependence $\Sigma_{xc}(\mathbf{r}, \mathbf{r}', \omega)$, but also by its dependence on the energy ω . This leads, in particular, to an additional mass renormalization of quasi-particles and to damping due to the imaginary part of $\Sigma_{xc}(\mathbf{r}, \mathbf{r}', \omega)$. Thus, there is formally no reason to identify the electronic band spectrum described by the Kohn–Sham equation (58) with the real spectrum of one-electron excitations in a metal. Such attempts were, however, made long ago. The majority of theoreticians, especially those engaged in the many-body problem and in the application of field theory methods in solid state physics, showed and now show an exceptionally skeptical attitude towards such attempts. This skepticism was most vividly expressed by M Norman [19] at the 1991 ‘Fermiology of HTSC Systems’ Conference held at the Argonne National Laboratory. The proceedings of this conference were published in [67]. The passage from Norman’s concluding talk is presented in Fig. 6.

As follows, among other things, from Norman’s views cited in the figure, the DFT band spectrum describes to good accuracy real Fermi surfaces even in HTSC systems. The situation with the majority of other investigated metals [63] is exactly the same or perhaps even somewhat better.

In identifying the DFT spectrum with a real excitation spectrum of a system of interacting electrons in a rigid lattice, one can, ignoring the ill feeling of colleagues, go farther than simply establish the form of the Fermi surface. Using the Kohn–Sham equation, one can calculate the optical and kinetic characteristics of metals, as well as EPI matrix elements and EPI spectral densities. Such attempts have also been made for a long time. Without derogating the merits of other researchers in this field (the references can be found in our original papers [51, 61, 68–70]), we find it more convenient to present here the results of our own studies for they include calculations for a large number of metals.

Considering the Kohn–Sham equation as a standard one-particle equation for electronic excitations, one can readily write the expression for the dielectric function $\varepsilon(\omega)$ of such a system [69]:

$$\varepsilon(\omega) = \varepsilon_{\text{intra}}(\omega) + \frac{8\pi^2}{3m^2} \sum_{\mathbf{k}, \lambda, \lambda'} \frac{f_{\mathbf{k}\lambda}(1 - f_{\mathbf{k}\lambda'}) |P_{\lambda\lambda'}^{\mathbf{k}}|^2}{(\varepsilon_{\mathbf{k}\lambda} - \varepsilon_{\mathbf{k}\lambda'})^2 (\varepsilon_{\mathbf{k}\lambda'} - \varepsilon_{\mathbf{k}\lambda} - \omega - i\delta)}. \quad (64)$$

I was asked by someone at the conference to say something nice about band theory. The best thing I can say is that band theory is like a prostitute. You get what you can out of her, then spurn her afterwards (a certain member of the band theory community asked me afterwards whether this made him a pimp). This is not meant to be a derogatory statement, but to highlight that the many-body community feels free to take parameters from a band calculation to use in their favorite model, but deride the calculation itself as “one-electron theory only pursued by simpletons” (thus, perhaps rape is a better term than prostitution). The fact is, it is somewhat amazing how ignorant some members of the many-body community are about density functional theory after 30 years time (not to be bigoted, certain band theory practitioners also fall in this category). The eigenvalue spectrum has to be taken with a very large grain of salt (after all, they merely act as Lagrange multipliers in the energy functional). Despite this, it is rather intriguing to see that such a complicated Fermi surface as predicted by band theory for YBCO seems to be confirmed by various experiments discussed here. Angle-resolved photoemission, as reported by Veal and Campuzano, sees the two barrel sheets (bonding and antibonding combinations of the CuO double layers), positrons, as reported by Manuel and Smedskjaer, see the ridge sheet coming from the chains, and several dHvA experiments (Los Alamos, Tohoku, and Grenoble groups) claim to see the small zone corner piece (another chain-related feature).

Figure 6. Quotation from the talk by M Norman [19] illustrating the attitude of many theoreticians to the electronic band theory.

The first term here stands for the intraband contribution and the second, respectively, for the interband one. The quantity $P_{\lambda\lambda'}^{\mathbf{k}}$ specifies the matrix element of the optical-transition operator:

$$P_{\lambda\lambda'}^{\mathbf{k}} = \langle \psi_{\mathbf{k}\lambda'} | i\nabla | \psi_{\mathbf{k}\lambda} \rangle. \quad (65)$$

The intraband contribution can be written as the standard Drude formula

$$\varepsilon_{\text{intra}}(\omega) = 1 - \frac{\omega_{\text{pl}}^2}{\omega(\omega + i/\tau)}, \quad (66)$$

where the plasma energy ω_{pl} is described by formula (40). The relaxation rate $1/\tau$ can be found from the static electrical resistivity. Such an approach to the determination of $1/\tau$ is fairly justified when used to describe the optical spectra of most metals at room temperature. For HTSC systems, the approach to the calculation of the intraband contribution should be more rigorous, and we shall discuss it in the next section. Employing the energies $\varepsilon_{\mathbf{k}\lambda}$ and the wave functions $\psi_{\mathbf{k}\lambda}(\mathbf{r})$ obtained from the solution of the Kohn–Sham equation, one can calculate $\varepsilon(\omega)$ and all the optical characteristics of metals. The results of such calculations for Pd are presented in Fig. 7. The figure shows that this approach, despite the absence of any convincing direct proof of the possibility of its usage, leads to surprisingly good agreement for the optical spectra and the electron energy loss spectra $L(\omega) \sim -\text{Im}[1/\varepsilon(\omega)]$ both for simple and transition metals. It has recently been shown [71] that the results of calculations for Pd can be significantly improved by the use of the theory of the time-dependent density functional [72]. This approach allows for the dependence of the exchange-correlation potential $V_{\text{xc}}(\mathbf{r})$ on the density n which in the presence of an alternating external field depends in turn on both the coordinates and time, $n(\mathbf{r}, t)$. Our detailed calculations [70] have shown that the optical spectra of a large number of simple and transition metals, including some magnetic metals, are described in this approach with almost the same accuracy as for Pd. Furthermore, the magneto-optic characteristics of metals were also shown [73] to be rather well described with the help of the DFT spectra of metals.

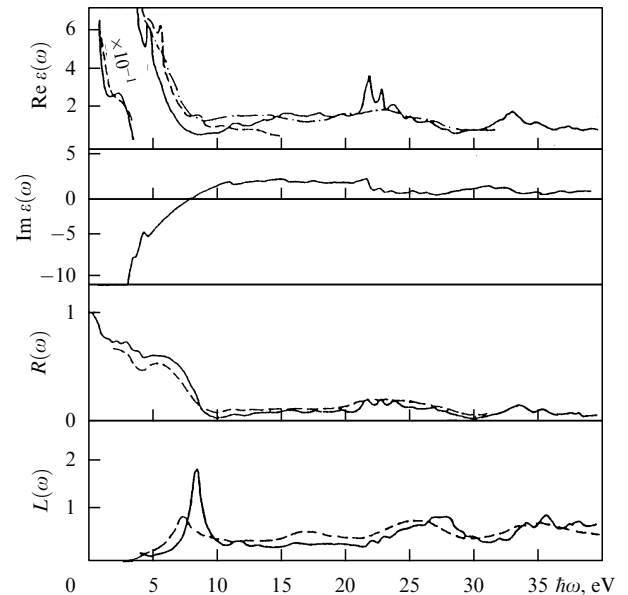


Figure 7. Optical spectra of palladium. The solid curves show theoretical data, the others give experimental values. $R(\omega)$ is the reflection coefficient.

Attempts have repeatedly been made (see [60] and the references in [51]) to calculate the matrix element and spectral densities of EPI by considering the Kohn–Sham equation as a standard one-electron operator. The idea of these calculations is rather simple. The matrix element is written as

$$g_{\mathbf{k}\mathbf{k}'} \approx \int d\mathbf{r} \psi_{\mathbf{k}'\lambda} \nabla V_{\text{eff}}(\mathbf{r}) \psi_{\mathbf{k}\lambda}, \quad (67)$$

where the effective potential has the form

$$V_{\text{eff}}(\mathbf{r}) = \sum_n V_n(\mathbf{r} - \mathbf{R}_n) + e \int \frac{n(\mathbf{r}') d\mathbf{r}'}{|\mathbf{r} - \mathbf{r}'|} + V_{\text{xc}}(\mathbf{r}). \quad (68)$$

For further calculations, experimental phonon spectra were normally used. This one-particle approach has recently been extended [74, 75] to a self-consistent calculation of both the

phonon spectra of metals and the EPI matrix elements. The main difference of this method from the previous calculations is the use of the linear response theory in calculation of the electron density variation under nuclear displacement corresponding to one or other phonon mode. In particular, the expression for EPI matrix element within this approach can schematically be represented as

$$g_{\mathbf{k}\mathbf{k}'\lambda\lambda'} = \int d\mathbf{r} \psi_{\mathbf{k}'\lambda'}^* \delta V_{\text{eff}}(\mathbf{r}) \psi_{\mathbf{k}\lambda}, \quad (69)$$

where

$$\begin{aligned} \delta V_{\text{eff}}(\mathbf{r}) = & \sum_n \nabla_n V_n(\mathbf{r} - \mathbf{R}_n) + e^2 \sum_n \int \frac{\nabla_n \delta n(\mathbf{r}')}{|\mathbf{r} - \mathbf{r}'|} d\mathbf{r}' \\ & + \sum_n \frac{\delta V_{\text{xc}}(\mathbf{r})}{\int \delta n(\mathbf{r}')} \nabla_n \delta n(\mathbf{r}') d\mathbf{r}'. \end{aligned} \quad (70)$$

The change in the electron density has the form

$$\delta n(\mathbf{r}) = \sum_{\mathbf{k}, \lambda}^{\varepsilon_F} (\psi_{\mathbf{k}\lambda}^0(\mathbf{r}) \delta \psi_{\mathbf{k}\lambda}(\mathbf{r}) + \text{c.c.}). \quad (71)$$

The quantity $\delta \psi_{\mathbf{k}\lambda}(\mathbf{r})$ is calculated using the Sternheimer method [76] which consists in the numerical solution of the inhomogeneous Kohn–Sham equation. This method is presented in detail in our review [51], and we shall not touch upon it here. Figure 8 gives the results of our calculations of the Eliashberg function for Nb which, as in the case of optical spectra, demonstrate a very good agreement with experiment. The difference of the function $\alpha^2(\omega)F(\omega)$ for Nb in the region of the second peak is due rather to the drawbacks of experimental measurements than the theoretical calculation. One should remember that all these calculations are carried out without employing any adjustable parameters. In fact, only the number of the element in the periodic table is used.

Concluding this section, we shall briefly summarize the consideration of the question of what a conventional metal is. First of all, a conventional metal is such a metal whose electron subsystem in a rigid lattice is well described by the

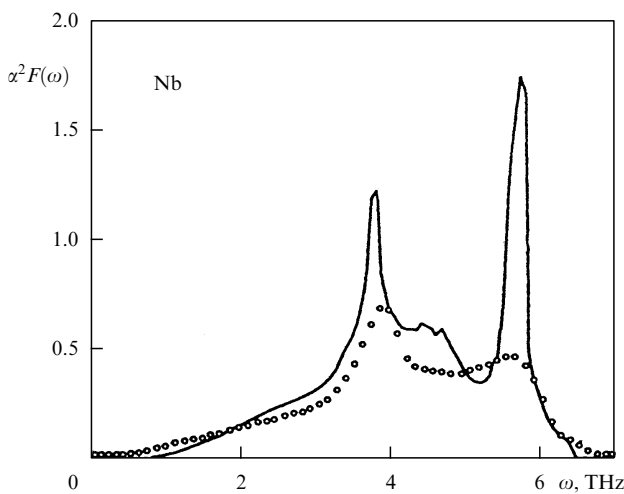


Figure 8. Eliashberg function for Nb. The solid curve represents calculations and the points correspond to experimental data.

Landau Fermi-liquid theory. Furthermore, the very parameters of this theory are rather well specified using the electronic band theory based on DFT. Unfortunately the above-mentioned facts cannot be accurately and rigorously grounded, but they can be easily confirmed by direct numerical calculation of the corresponding properties of metals. Possible reasons for such behavior of conventional metals can be found from studies of a homogeneous electron gas [77, 78], where the exchange-correlation self-energy part $\Sigma_{\text{xc}}(\mathbf{k}, \omega)$ in the range of densities corresponding to those of real metals was shown to be a very smooth function of \mathbf{k} and ω changing strongly only for $\Delta k \sim k_F$ and $\Delta \omega \sim \varepsilon_F$.

3. How far are superconducting cuprates from ‘conventional’ metals?

Proceeding to the discussion of the properties of cuprates with high T_c values, we have to note first of all that we shall mainly deal with optimally doped compositions. First, because these systems are most often considered as unconventional metals that demonstrate non-Fermi-liquid behavior and various anomalies. Second, as we shall try to show at the end of this section, the behavior of underdoped and overdoped HTSC systems is in fact much farther from the behavior of ‘conventional’ metals considered above. We shall begin the discussion with the results of calculations of the electronic band structure.

As has been mentioned above, the Fermi surfaces of HTSC metals calculated within DFT are in good agreement with experimental data. This follows both from our own calculations [79] and those reported by a large number of other research groups (see review [80] and references therein). A detailed analysis of this problem was presented in the talks at the above-mentioned meeting at the Argonne National Laboratory [67]. A good coincidence of Fermi surfaces proves that even if the exchange-correlation effects in these systems are strong, they do not lead to strong spatial nonlocality of the exchange-correlation self-energy part of the one-particle Green function. This fact follows immediately from comparison of the Kohn–Sham equation (58) and equation (62) which specifies a Fermi surface. This means in turn that if the behavior of optimally doped systems shows up some serious peculiarities, they are mostly determined by the energy dependence of $\Sigma_{\text{xc}}(\mathbf{r}, \mathbf{r}', \omega)$.

For a number of HTSC systems, optical characteristics were also calculated [81–85] on the basis of the electronic band structure, the calculation procedure being exactly the same as described in the preceding section for conventional metals. Calculations performed by different groups slightly disagree because unlike methods were employed, but the variance is small enough. In what follows we shall present the results of our calculations [81–83] as they underwent a much more thorough comparison with experimental data both in our own works and in the works by experimentalists.

Figure 9 presents the results of our calculations [81] of the imaginary part of the dielectric function $\text{Im} \varepsilon(\omega)$ for $\text{La}_{1.84}\text{Sr}_{0.16}\text{CuO}_4$ and the experimental data for this function obtained by the Japanese group [86]. As noted in the experimental paper [86], the theoretical and measured values of $\text{Im} \varepsilon(\omega)$ for energies $\omega \gtrsim 2$ eV show an almost perfect coincidence. This makes it possible to determine from theoretical calculations such an important characteristic of HTSC systems as $\varepsilon(0)$ which is the contribution of high-energy interband transitions to the low-energy ($\omega < 1$ eV)

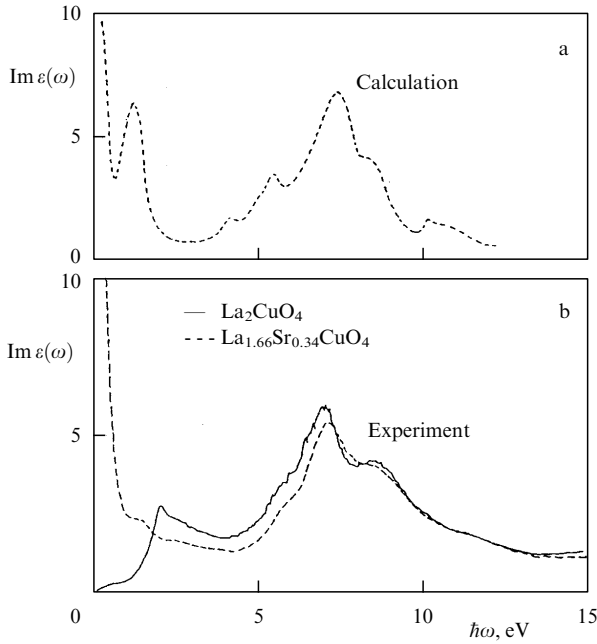


Figure 9. Comparison of the experimental data [86] (b) with the results of the calculations [81] (a) for the imaginary part of the dielectric permittivity.

electron polarizability:

$$\epsilon(0) \approx 1 + \int_{3 \text{ eV}}^{\infty} \frac{\text{Im} \epsilon(\omega')}{\omega'} d\omega'. \quad (72)$$

In the majority of superconducting cuprates this quantity is sufficiently large, $\epsilon(0) \sim 6-10$. We would like to point out the intense interband transition for $\omega \approx 1 \text{ eV}$, obtained in our calculations. Traces of this transition for the same energies are also seen on the experimental curves. In our calculations the peak intensity is certainly overestimated, which can readily be explained: these calculations were carried out rather long ago on a poor computer using a small number of \mathbf{k} -points in the integration over the Brillouin zone. A much more detailed consideration was given to the optical spectra of $\text{YBa}_2\text{Cu}_3\text{O}_7$ by several research groups. We shall now proceed to a detailed discussion of these results.

First of all, we would like to specify some points of our preceding discussion of calculation of the optical spectra of metals. Up to now we have considered the dielectric function $\epsilon(\omega)$ and the optical conductivity $\sigma(\omega)$ as scalar functions of energy. This is actually correct for cubic crystals. Our above-mentioned calculations for simple and transition metals were performed for this particular structure. Superconducting cuprates possess either tetragonal or even orthorhombic symmetry. For these, both $\epsilon(\omega)$ and $\sigma(\omega)$ are tensors $\epsilon_{\alpha\beta}(\omega)$ and $\sigma_{\alpha\beta}(\omega)$ which can be diagonalized. So, for tetragonal symmetry we have

$$\epsilon_{xx}(\omega) = \epsilon_{yy}(\omega) \neq \epsilon_{zz}(\omega), \quad (73)$$

and for orthorhombic symmetry —

$$\epsilon_{xx}(\omega) \neq \epsilon_{yy}(\omega) \neq \epsilon_{zz}(\omega). \quad (74)$$

Here the z axis is assumed to be aligned with the c axis perpendicular to CuO planes. The transport processes along

the z axis are of course not described with good accuracy in the electronic band theory. This question is very important and interesting, but its discussion deviates from the theme of this review. Formally, components of the dielectric function and optical conductivity tensors are calculated in the same way as for cubic crystals, but with replacement of the optical transition operator ∇ in (65) by respectively $\partial/\partial x$, $\partial/\partial y$, and $\partial/\partial z$.

Figure 10 presents the results of our calculations [82, 83] of the reflection coefficient in the CuO plane for $\text{YBa}_2\text{Cu}_3\text{O}_7$ together with the experimental data obtained for films of this compound. It should be noted that the theoretical and experimental results are on the whole in good agreement. Our calculations were naturally carried out for the single crystal and demonstrate the fairly strong anisotropy of the reflection factor along a and b axes. Here the b axis is directed along the chains consisting of Cu and O atoms and the a axis is perpendicular to them. The films in the experiments did not show a distinguished direction for chains because of twinning effects. In Figure 11 we present the results of our calculations [82, 83] of the function $L(\omega) \sim -\text{Im}[1/\epsilon(\omega)]$ which describes the energy loss spectrum in a crystal. The agreement between the experimental and theoretical values for this function is also rather good, at least not worse than for any transition metal. We should emphasize the good coincidence between experiment and the calculations in the description of the low-frequency plasma oscillation due to conduction electrons for $\omega \approx 1 \text{ eV}$. The function $L(\omega)$ was measured for most of the cuprates [90], and its form differs little from compound to compound. The $L(\omega)$ curve shows two distinct singularities. These are, first, the low-frequency plasma oscillation of valence electrons for $\omega \sim 1 \text{ eV}$ in all metallic compounds and, second, a strongly developed spectrum of charge density fluctuations stretching from energies $\omega \sim 2 \text{ eV}$ to $\omega \sim 40-50 \text{ eV}$. Such a density fluctuation spectrum leads to high values of the static dielectric constant $\epsilon(0) \sim 6-10$ and, therefore, to a strong screening of the Coulomb interaction.

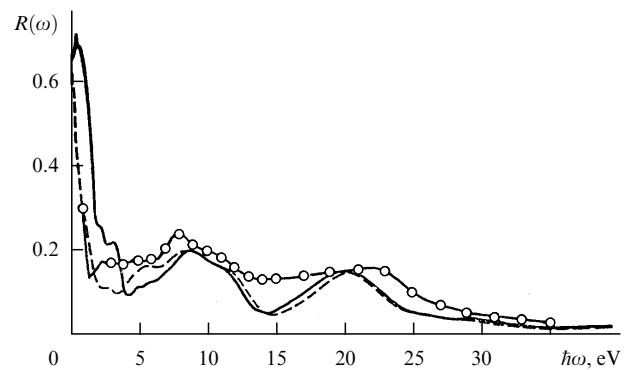


Figure 10. Reflection coefficient of $\text{YBa}_2\text{Cu}_3\text{O}_7$ in the energy range of 0–40 eV: the solid line gives the calculation for $\mathbf{E}||b$, the dashed line — the calculations for $\mathbf{E}||a$, and the solid line with circles corresponds to the experimental data [87].

Figure 12 is a plot of the calculated reflection coefficient [82] for YBCO along the a and b axes for a smaller energy interval than that of Fig. 10, which makes a comparison with the experimental data obtained with twin-free single crystals [91–94] easier. Well pronounced in Fig. 12 is the strong anisotropy of the reflection coefficient along the a and b axes, which is clearly observed in the experiments as well. The most

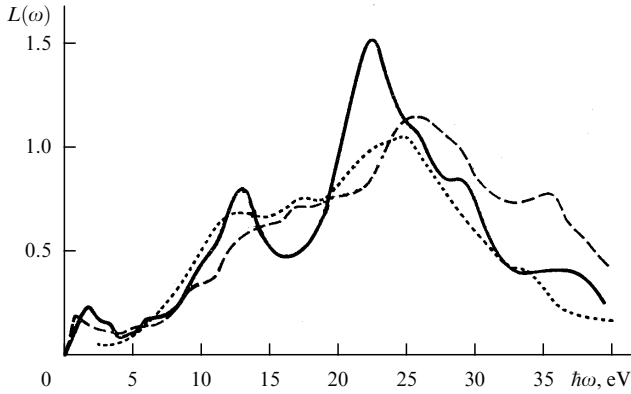


Figure 11. Function of the characteristic energy loss of $\text{YBa}_2\text{Cu}_3\text{O}_7$. The solid line is for the calculations [82, 83], the dashed line — for the experiment [88], and dotted line — for the experiment [89].

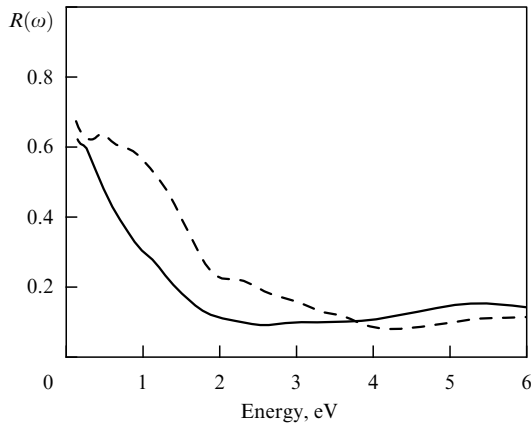


Figure 12. Reflection coefficient of $\text{YBa}_2\text{Cu}_3\text{O}_7$ [82] in the energy range up to 6 eV. The solid curve is for $\mathbf{E}||a$ and the dashed curve — for $\mathbf{E}||b$.

detailed comparison of experimental data with our calculations [82, 83] was undertaken by the Zürich group [91]. They reported a surprisingly good general agreement between the experimental and theoretical data on the anisotropy of the reflection coefficient, including even the intersection of $R(\omega)$ curves for energies $\omega \sim 3-4$ eV. Moreover, their paper examined in detail the interband transitions revealed in our calculations. The most intense of these transitions, the one for $\omega \approx 0.4$ eV, is also clearly pronounced on the curve of reflection along the b axis. The presence of an intense interband transition in the b direction, i.e., in CuO chains, for energies $\omega \approx 0.4$ eV was noted in the early paper by the Leningrad group [92]. The existence of all interband transitions calculated by us in the energy range under $\omega \sim 4$ eV was confirmed in paper [91]. The only difference is that in experiments the interband transition in the plane (i.e., along the a axis) for energies $\omega \sim 0.6$ eV has a somewhat higher intensity than follows from our calculations. The general conclusion drawn in paper [91] is that the optical spectra of an optimally doped YBCO system are very well described within the standard electronic band theory at least for energies $\omega \gtrsim 0.5$ eV.

In the range of low energies, the situation is much less rosy. In our calculations [81–83] we described the intraband transitions using the simplest approximation, namely, the

standard Drude formula for conductivity:

$$\sigma(\omega) = \frac{\omega_{\text{pl}}^2}{4\pi} \frac{1}{-i\omega + 1/\tau}. \quad (75)$$

The plasma frequency ω_{pl} was calculated on the basis of the electronic band structure, and the magnitude of the relaxation rate was determined from comparison with static electrical resistivity. This approach worked adequately for the simple and transition metals investigated by us before. In cuprates, however, the simple Drude formula (75) does not at all describe the experimental data. In one of the early experimental investigations [94] of the optical spectra of $\text{YBa}_2\text{Cu}_3\text{O}_7$ single crystals it was noted that the low-energy behavior of the reflection coefficient $R(\omega)$ and the optical conductivity $\sigma(\omega)$, which are due to the reflection of light from the CuO plane, is rather well described by the generalized Drude formula with a frequency-dependent effective mass $m^*(\omega)/m$ and relaxation rate $1/\tau(\omega)$. It was also pointed out that the quantity

$$\frac{1}{\tau^*(\omega, T)} = \frac{1}{\tau(\omega, T)} \frac{m}{m^*(\omega, T)}$$

demonstrates an unusual, according to the authors of [94], linear dependence on ω up to energies $\omega \sim 2000 \text{ cm}^{-1}$ (0.25 eV). Such a behavior of the function $1/\tau^*(\omega)$ was customarily identified, both by the authors themselves and by many other researchers, with the non-Fermi-liquid behavior of electrons in HTSC systems. The ‘marginal’ Fermi liquid [95], the Luttinger liquid and the ‘nesting’ type peculiarities of an electron spectrum [25] were considered as possible models of such a behavior of the relaxation rate. We showed rather long ago [96] that the data reported in paper [94] can quite naturally be explained in the framework of the strong EPI model.

Our calculations were carried out according to the following scheme. To calculate the intraband contribution to the dielectric function (DF), we used the expression

$$\varepsilon(\omega) = \varepsilon(0) + \frac{4\pi i}{\omega} \sigma(\omega). \quad (76)$$

Here $\varepsilon(0)$ is the contribution of interband transitions to the low-energy part of DF. We obtained its value $\varepsilon(0) \sim 8$ earlier using the electronic band structure calculations. For the optical conductivity $\sigma(\omega)$ we employed the generalized Drude formula (35). According to the *ab initio* calculations [82] and the analysis of the experimental data [97], the plasma energy of electrons was chosen to be 3 eV. Unfortunately, no comprehensive data on the transport spectral density of EPI necessary for the calculation of optical conductivity are available. For this purpose we used a function of the form $\alpha_{\text{tr}}^2(\omega)F(\omega)$ which gives a rather reasonable density of phonon states in HTSC systems [98]. This function is plotted as a solid line in Fig. 13. The only adjustable parameter in the procedure is thus the EPI constant

$$\lambda_{\text{tr}} = 2 \int_0^\infty \frac{\alpha_{\text{tr}}^2(\omega)F(\omega)}{\omega} d\omega.$$

The best agreement with experimental data is obtained for $\lambda_{\text{tr}} = 2.1$. The same Fig. 13 presents the results for $\alpha_{\text{tr}}^2(\omega)F(\omega)$ obtained from calculations of $\sigma(\omega)$ according to formula (54)

from the preceding section:

$$\alpha_{tr}^2(\omega)F(\omega) \sim \frac{d^2}{d\omega^2} \left[\omega \operatorname{Re} \frac{1}{\sigma(\omega)} \right].$$

As can be seen from Fig. 13, even at rather low temperatures ($T = 10$ K) this formula poorly reproduces the function $\alpha_{tr}^2(\omega)F(\omega)$. At higher temperatures ($T = 100$ K), the situation is even worse. A very rough idea of the spectral density of EPI can be derived from experimental data on conductivity with the help of this formula because for $T < 93$ K the investigated system is in the superconducting state. Somewhat better results can be obtained from the solution of the inverse problem of the reconstruction of this function from the solution of the integral equation for the function $1/\tau_{tr}(\omega)$ or directly from the reflection coefficient $R(\omega)$. This point is to be discussed later.

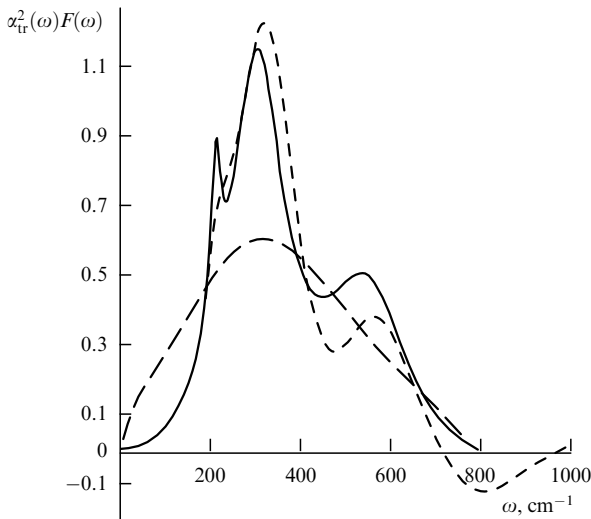


Figure 13. Transport spectral function. The solid curve is the model function $\alpha_{tr}^2(\omega)F(\omega)$, the dashed curve is the function obtained according to (54) for $T = 10$ K, and the long-dashed curve is for $T = 100$ K.

We have recently undertaken [99] a more thorough examination of the frequency and temperature dependences of the optical reflection coefficient in the YBCO system. For the analysis we used the experimental data obtained by Nicole Bontemps's group with high-quality YBCO films. For the calculation we exploited the same approach as that described above. The only difference was that the contribution of interband transitions in the IR spectral region was added to formula (76) for DF. This contribution had the form of a broad Lorentzian:

$$\varepsilon_{inter}(\omega) = \frac{\omega_{in}^2}{\omega_c^2 - \omega^2 + i(\omega/\tau_c)}. \quad (77)$$

The following values of parameters were used in equation (77): $\omega_{in} = 6000 \text{ cm}^{-1}$, $\omega_c = 5800 \text{ cm}^{-1}$, and $1/\tau_c = 9000 \text{ cm}^{-1}$. These parameters were chosen in close accordance with our *ab initio* calculations for interband transitions in the YBCO system [82].

Figure 14 gives the results of calculations and the experimental data [99]. The value $\lambda = 2$ was used for the EPI constant. It is clearly seen in the figure that the strong EPI

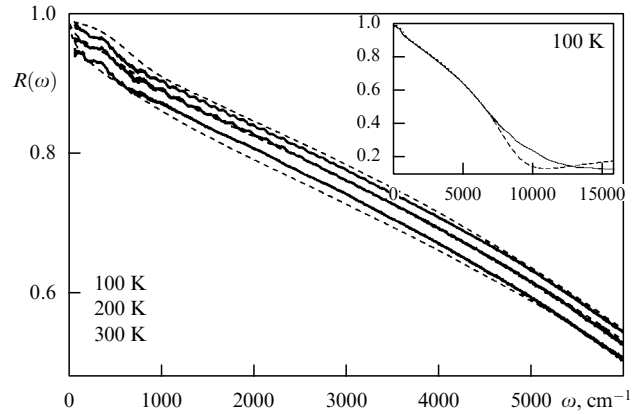


Figure 14. Measured (solid curve) and calculated (dashed curve) reflection coefficient for YBCO films. Downward: 100, 200, and 300 K. The inset shows the behavior of $R(\omega)$ over a wider energy range.

model reproduces commendably both the frequency and temperature dependences of the reflection coefficient for an YBCO film over broad energy (up to 6000 cm^{-1}) and temperature ranges. A comparison of the theoretical calculations and the experimental data at $T = 300$ K over a wider energy range is shown in the inset. Some discrepancy in these data for $\omega > 1 \text{ eV}$ is seen, but it can easily be eliminated by a more accurate account of the interband transitions for energies $\omega \sim 1 \text{ eV}$. It should be noted that this approach also excellently describes the static electrical resistivity $\rho(T)$ of these films, which increases linearly with temperature for $T > T_c$. Moreover, even the agreement with the absolute value of $\rho(T)$ is very good.

It is commonly stated that the relaxation rate $1/\tau_{tr}^*(\omega)$ grows linearly in HTSC systems with increasing energy ω up to $\omega \sim 1 \text{ eV}$. The strong EPI model cannot naturally cause such behavior of $1/\tau_{tr}^*(\omega)$, which can be readily verified from the results of the calculation of this quantity presented in the preceding section. It actually has a quasi-linear dependence on ω below $\omega \sim (2-3) \omega_{max}$ and then it grows much more slowly tending to saturation for $\omega \sim (8-10) \omega_{max}$, where ω_{max} is the maximum phonon energy equal to $\sim 0.1 \text{ eV}$ (800 cm^{-1}). The significant difference of HTSC systems from the majority of other metals is associated with the absolute values of $1/\tau(\omega, T)$. So, even in the static limit, where

$$\frac{1}{\tau(0, T)} \simeq 2\pi\lambda T$$

its value reaches $\approx 0.1 \text{ eV}$, which exceeds more than tenfold the temperature value itself. Such high $1/\tau(\omega)$ values have recently been observed in the photoemission measurements [100].

In the analysis of experimental data on the behavior of $1/\tau(\omega)$ in the YBCO system [25, 101], the intense interband transitions in the IR spectral region are often disregarded. This circumstance, as shown in our paper [96], entails a fictitious increase of $1/\tau_{tr}^*(\omega)$ precisely due to the interband transitions.

In this context, the studies of bismuth [102] and thallium [103] cuprates appear to be much more informative for the analysis of the frequency dependence of $1/\tau(\omega)$. Although no *ab initio* calculations of the optical spectra of these com-

pounds have been made to the best of our knowledge, one can conclude even from the electron spectra calculated for them that the existence of intense interband transitions is highly improbable in the IR region of their spectrum. Figure 15 presents the graphs of the energy dependence of the effective mass $m_{tr}^*(\omega)/m$ and the relaxation rate $1/\tau_{tr}^*(\omega)$ for $\text{Bi}_2\text{Sr}_2\text{CaCu}_2\text{O}_6$ as published in [102]. These results clearly indicate that neither the marginal Fermi liquid theory [95], nor the Luttinger liquid theory [101] can describe them over a reasonably broad energy range. Figure 16 shows perfect agreement with experiment for $m_{tr}^*(\omega)/m$ and $1/\tau_{tr}^*(\omega)$ calculated [104] within the model of strong EPI with the coupling constant $\lambda = 1.9$. Similar results for $1/\tau_{tr}^*(\omega)$ were obtained for thallium compounds as well [103].

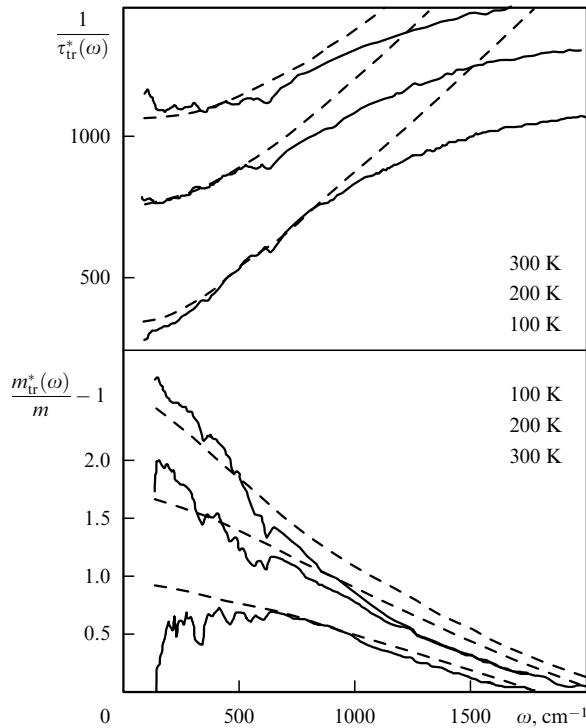


Figure 15. Relaxation rate and effective mass for BSCCO. The solid curve gives experimental data and the dashed curve — the calculation within the theory of marginal Fermi liquid.

The results of calculations and their comparison with experimental data, which we presented above, convincingly demonstrate, in our opinion, not only the possibility of explaining the properties of the normal state of optimally doped systems using the strong EPI model, but also the actual validity of this model. The only alternative to EPI for the description of relaxation processes might be the interaction among electrons and spin fluctuations. This approach was developed by the group headed by D Pines [21, 22] and is supported by a large number of other researchers engaged in the study of HTSC systems. It will be shown now that in actuality the interaction of electrons with spin fluctuations cannot in principle explain the relaxation of charges and currents in HTSC systems. First of all, as follows from the preceding consideration, the excitations with energies $\omega \lesssim (5-6)T_c$ responsible for the electron relaxation must exist to explain the linear dependence of electrical resistivity for $T > T_c$ and the temperature- and frequency-dependences

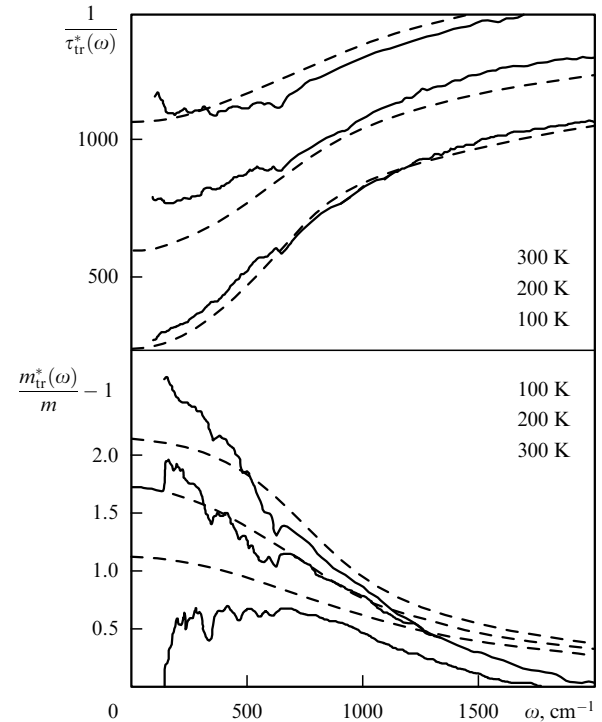


Figure 16. Relaxation rate and effective mass for BSCCO. The solid curve is the same as in Fig. 15. The dashed line is the calculation in the strong EPI model.

of the relaxation rate. It is quite clear that the greater part of the phonon spectrum in HTSC systems satisfies this condition. The solution of the inverse problem of the intermediate-boson spectrum reconstruction from experimental data on the reflection (or absorption) coefficient in HTSC systems and heavy-fermion systems was given in paper [105]. The paper reported a close coincidence between the spectrum of intermediate bosons responsible for electron relaxation and the phonon spectrum in HTSC systems. In heavy-fermion systems, this spectrum coincides with low-energy ($\omega \sim 10 \text{ cm}^{-1}$) spin fluctuations. An analogous result was obtained [104] from the solution of the inverse problem for the function $1/\tau(\omega)$ obtained for BSCCO in the above-mentioned experimental paper [102]. Since the inverse problem was solved for the normal-state spectra, i.e., for sufficiently high temperatures, the calculated spectrum of intermediate bosons does not reproduce the details of the actual spectrum of phonons or any other excitations. It rather resembles the result obtained by a differentiation of $\omega \text{Re}[1/\sigma(\omega)]$, which appears as the dashed line in Fig. 13. Nonetheless, this procedure allows a correct reconstruction of a few first moments of the function $\alpha_{tr}^2(\omega)F(\omega)$, including the coupling constant λ_{tr} and the mean effective energy of these bosons

$$\bar{\omega} = \frac{2}{\lambda_{tr}} \int_0^{\infty} \alpha_{tr}^2(\omega) F(\omega) d\omega. \quad (78)$$

The most significant result of this analysis, besides the fact that the spectrum of intermediate bosons lies in the same energy range as the phonon spectrum, is the proof of the existence of high values of the coupling constant with intermediate bosons, $\lambda_{tr} \approx 2$, in HTSC systems. Practically the same result was obtained in the recent paper [106]. The

coupling constant λ calculated in [106] appeared to be even greater than ours, $\lambda_{tr} = 2.6$. True, the authors of [106] associated their spectrum with spin fluctuations. The impossibility of coupling constants $\lambda_{tr} \sim 2$ for spin fluctuations becomes obvious from considerations, of the type of those presented in the introduction, concerning the role of the residual quasi-particle interaction. Since the static electrical resistivity in HTSC systems demonstrates a linear temperature-dependence from $T = T_c$ and on, the relaxation rates for both EPI and the interaction with spin fluctuations can formally be written as

$$\frac{1}{\tau_{ph}} = 2\pi\lambda_{ph}T \quad (79)$$

and

$$\frac{1}{\tau_{sp}} = 2\pi\tilde{\lambda}_{sp}T. \quad (80)$$

The coupling constant with spin fluctuations determining the linear dependence $\rho(T)$ can be written in the form [21, 31, 109]

$$\tilde{\lambda}_{sp} = 2 \sum_{\mathbf{q}} \int_0^T \frac{d\omega}{\omega} g_{sp}^2 \text{Im} \chi(\mathbf{q}, \omega). \quad (81)$$

Here g_{sp} is the matrix element of the interaction among electrons and spin fluctuations, and $\chi(\mathbf{q}, \omega)$ is the magnetic susceptibility of the conduction electrons.

It is more convenient to rewrite $\tilde{\lambda}_{sp}$ in the form

$$\tilde{\lambda}_{sp} = \lambda_{sp} \frac{\tilde{n}_s}{n_s}, \quad (82)$$

where λ_{sp} is the total coupling constant of electrons with spin fluctuations. It is specified by the same expression as (81), but with the energy integral going to infinity. This coupling constant λ_{sp} determines, in the model of spin fluctuations, the value of the critical temperature of a superconducting transition for d-pairing [21]. The quantity n_s specifies the total number of spins in the conduction band in the CuO plane:

$$n_s \sim \sum_{\mathbf{q}} \int_0^\infty d\omega \text{Im} \chi(\mathbf{q}, \omega). \quad (83)$$

In HTSC systems $n_s \sim 1$. The quantity \tilde{n}_s determines the number of spin excitations in the energy range up to $\omega \sim T$:

$$\tilde{n}_s \sim \sum_{\mathbf{q}} \int_0^T d\omega \text{Im} \chi(\mathbf{q}, \omega). \quad (84)$$

Spin fluctuations observed, for example, with the help of neutron scattering actually exist in HTSC systems. In particular, the peak of the function $\text{Im} \chi(\mathbf{q}, \omega)$ is observed for $\omega \approx 30$ meV and the wave vector $\mathbf{q} = (\pi, \pi)$ corresponding to the period of the antiferromagnetic ordering in the $\text{YBa}_2\text{Cu}_3\text{O}_7$ system. These antiferromagnetic fluctuations may in particular be responsible for the anomalous behavior of the relaxation time of the nuclear magnetic spin on Cu nuclei [21, 22]. A detailed examination of the function $\text{Im} \chi(\mathbf{q}, \omega)$ up to energies $\omega \sim 30$ meV and for a large number of wave vectors \mathbf{q} was undertaken in paper [109]. It was shown using the sum rule (82) that for the indicated energy range ($\omega \lesssim 30$ meV) the value of \tilde{n}_s is only 3.2% of the total number of spins n_s . The most optimistic estimates following from the

model of d-pairing due to spin fluctuations give the total coupling constant $\lambda_{sp} \lesssim 1$, which suggests that the spin fluctuations are unable to explain either the absolute values of the optical relaxation rate $1/\tau(\omega)$ or its temperature and frequency dependence. In order that the optical relaxation due to spin fluctuations could be described, their whole spectrum must be displaced to the low-energy region $\omega \lesssim 0.1$ eV, as follows from what has been said above, including the numerical solutions of the inverse problem of the intermediate-boson spectrum reconstruction [104–106]. Such ‘softening’ of the whole spectrum of spin fluctuations seems to have no physical grounds.

Thus, in our opinion the above discussion unambiguously suggests the conclusion that the properties of the normal state of optimally doped HTSC systems differ little from the properties of many other ‘conventional’ metals. Remembering the promise, given in the introduction, ‘not to juggle with facts or sweep the dust under the rug’, we now have to make some remarks to show that everything is not so simple even in optimally doped phases.

First of all, as we and many other authors have already pointed out, the measured Fermi surfaces in cuprates are well described by the theory of electronic band structure [67]. Papers have recently appeared that cast doubt on this assertion [110, 111]. The Fermi surface of BSCCO was measured again, this time by angle-resolved photoemission using incident photons with an energy of 33 eV. Up to the present time such measurements have made use of lower-energy photons. The results of these measurements are presented in Fig. 17. Figures 17 a, c show the dependence of the electron energy on the momentum $\varepsilon(\mathbf{k})$ and the form of the Fermi surface obtained in earlier experiments. Figures 17 b, d give the same quantities, but obtained using photons with an energy of 33 eV. As is seen from the figure, the new Fermi surface and the electronic spectrum differ substantially from those assumed before. First, the Fermi surface transforms from open to closed and, second, the so-called generalized

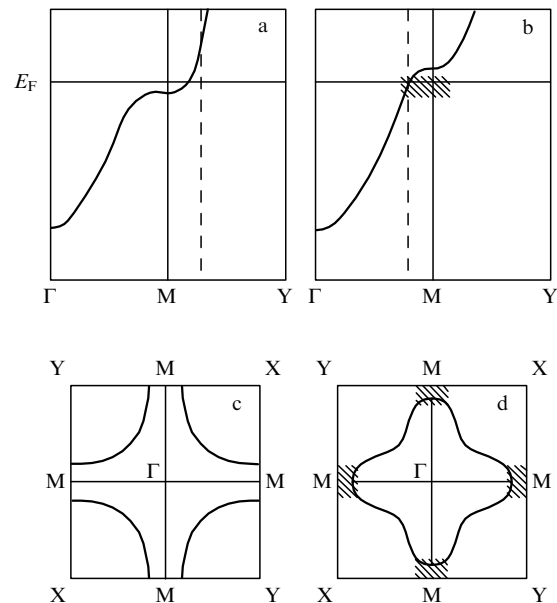


Figure 17. Schematic picture of the electron energy $\varepsilon(\mathbf{k})$ (a, b) and the Fermi surface (c, d) in BSCCO; (a, c) are previous views; (b, d) are the new results. The hatched areas in figures (b, d) are additional (non-bulk) states.

saddle point under the Fermi surface, which is actively used in many theories of HTSC systems, disappears. Figures 17 b, d account for the differences in the electron spectrum when photons of different energies are used in measurements. According to the authors of Refs [110, 11], photons of lower energy excite the surface or some other states not referring to the states of conduction electrons, which mask the actual form of the Fermi surface near the point M of the Brillouin zone. It is not yet time to discuss in detail the consequences that the existence of a closed Fermi surface will have for many theories of HTSC systems because the results of these measurements themselves were put in question in quite recent papers [112, 113].

One more difficult problem in HTSC systems arose after the observation in [114] of a linear increase of resistivity with temperature in the compound $\text{Bi}_2\text{Sr}_2\text{CuO}_x$ beginning right from T_c . The whole nontriviality of this dependence lies in the fact that the T_c value for this system is equal to 7 K! This example has since then been used as the principal argument in the proof of non-Fermi-liquid behavior of HTSC systems. It is noteworthy that a paper by another group [115] was simultaneously published which reported a linear growth of resistivity in the system $\text{Bi}_2\text{Sr}_2\text{CuO}_x$ beginning from much higher temperatures. This situation was experimentally examined at length in the paper by Vedenev et al. [116]. They showed that in high-quality single crystals with $T_c \approx 5$ K, the resistivity demonstrates the standard behavior described by the Bloch–Grüneisen formula with Debye temperature $\Theta_D \approx 270$ K. But this is only half the truth. The other half is that there exist samples of somewhat worse quality but with higher $T_c = 10$ K which do possess a linear dependence $\rho(T)$ up to $T_c = 10$ K. It is somehow very hard to believe that with an insignificant worsening of single crystal quality and a slight increase of T_c the electron system in $\text{Bi}_2\text{Sr}_2\text{CuO}_x$ transforms from a Fermi liquid to a Luttinger liquid. The above-described standard approach to an EPI system clearly fails to account for the linear dependence $\rho(T)$ up to $T \sim 10$ K. It should be noted, however, that transport processes in two-dimensional systems exhibiting strong electron–phonon interaction and interaction with impurities and defects have not yet been completely investigated [117]. The solution of the problem of ‘superlinear’ behavior of $\rho(T)$ in some $\text{Bi}_2\text{Sr}_2\text{CuO}_x$ samples should in our opinion be sought in some peculiarities of two-dimensional systems rather than in new physics.

The last problem in the list, but probably not the last in importance, which we shall briefly discuss at the end of this section is the strong anisotropy of relaxation times even in the normal state of optimally doped systems. This fact has recently been observed in experiments using angle-resolved photoemission. A number of papers discuss the nature of ‘hot’ and ‘cold’ points on a Fermi surface [118, 119] from the viewpoint of the spin fluctuation model. We should only like to emphasize here (a more extensive consideration is given in the section to follow) that the electron–phonon interaction in these systems is also strongly anisotropic.

4. The enigma of the superconducting state in cuprates

The first thing to be pointed out in this section is the possibility of explaining high values of the critical temperature of the superconducting transition in the framework of the strong EPI model considered above. If the distinctions

between the functions $\alpha_{\text{tr}}^2(\omega)F(\omega)$ and $\alpha^2(\omega)F(\omega)$ are neglected, which can normally be done for the majority of known metals, the solutions of the Eliashberg equations (42), (43) with the function $\alpha^2(\omega)F(\omega)$ depicted in Fig. 13 and the coupling constant $\lambda = 2$ gives $T_c = 93.1$ K. Slightly changing the function $\alpha^2(\omega)F(\omega)$ and increasing its intensity in the region of higher-energy phonons and also increasing the coupling constant a little to the value $\lambda = 2.3$, one can obtain $T_c = 125$ K. Thus, in spite of quite a number of pessimistic assertions, one can verify that the high T_c values in cuprates are by themselves not something unusual for strong EPI systems.

In many theoretical papers, the possible values of the EPI constant in high-temperature superconducting cuprates were estimated within DFT [120–124]. In these papers, it was not the total coupling constants λ that were typically calculated, but the coupling constants of electrons with certain phonon modes. The frequencies of those modes were determined by the method of ‘frozen’ phonons [61]. The main conclusion drawn in these papers is that there exist obvious physical reasons for the EPI in cuprates to be sufficiently strong. The estimates of the total coupling constant λ made in these papers yield values of the order of $0.6 \lesssim \lambda \lesssim 1.5$. The main reasons for the relatively large λ values in cuprates are as follows: first, their layered crystal structure which allows sufficiently high densities of electron states on the Fermi surface despite a rather small number of electrons per unit cell; second, the strong hybridization of the wave functions of electrons in Cu and O atoms on the plane, which allows even electrons bonded with a light oxygen atom to participate in EPI; and third, the considerable fraction of ionic bonding in these compounds. The absence of screening in the direction perpendicular to CuO planes leads to strong EPI on the plane because of the change of the Madelung potential on Cu and O atoms due to the phonons responsible for the motion of the apex oxygen ion and even Ba and Y ions in the $\text{YBa}_2\text{Cu}_3\text{O}_7$ system. The coupling constant with such modes is very large and reaches values $\lambda_v \sim 2-4$.

The spectral densities of EPI have been calculated [122, 125, 126] for a number of cuprates. We shall return to the discussion of these papers a little later, and now proceed to a consideration of experimental evidence of the strong EPI effects in the properties of the superconducting state of HTSC systems.

One such effect is a change in the phonon spectra of HTSC systems in the transition to the superconducting state. Such changes are observed in experiments on Raman scattering of light by optical phonons and the absorption of light by optically active phonons [127, 128], and also in neutron scattering experiments [98]. Particularly radical changes were observed [129] with the help of Raman scattering in the compound $\text{HgBa}_2\text{Ca}_3\text{Cu}_4\text{O}_{10+x}$ with $T_c = 123$ K. The changes in the phonon spectra are due to nonadiabatic effects caused by the electron–phonon interaction. Such effects were first predicted in paper [130] for the normal state of metal, and later they were also calculated for the superconducting state in the BCS model with isotropic pairing [131]. These effects are especially strong for optical phonons with small wave vectors \mathbf{q} ,

$$qv_F < \omega_0, \quad (85)$$

where v_F is the Fermi velocity and ω_0 is the nonrenormalized phonon frequency. In the region of wave vectors q specified

by condition (85), the nonadiabatic effects have no additional smallness besides the possible smallness of the coupling constant between a given mode and electrons [132]. For wave vectors $q > \omega_0/v_F$, nonadiabatic effects become small to the order of smallness of the ratio ω_0/ε_F in the normal state or the ratio Δ/ε_F in the superconducting state. This is the reason why the nonadiabatic effects are weakly pronounced in neutron experiments in which phonons with sufficiently large wave vectors \mathbf{q} are involved. However, as shown in paper [133], the situation may be essentially different in systems where ‘nesting’ is observed in the electron spectrum, and therefore strong nonadiabatic effects are possible for phonons with the wave vector \mathbf{q} coincident with the ‘nesting’ vector. Nonadiabatic effects are also observed in the normal state of metals possessing optical modes [134] where they may be substantial for HTSC systems for $T > T_c$ [132].

In all the above-mentioned experiments, the spectral density of the phonon Green function for the v th mode is in fact measured:

$$\text{Im } D_v(\mathbf{q}, \omega) = \frac{2\omega_0(\mathbf{q}) \text{Im } \Pi_v(\mathbf{q}, \omega)}{[\omega^2 - \omega_0^2(\mathbf{q}) - 2\omega_0(q) \text{Re } \Pi_v(q, \omega)]^2 + 4\omega_0^2(\mathbf{q}) \text{Im } \Pi_v^2(\mathbf{q}, \omega)}, \quad (86)$$

where $\Pi_v(\mathbf{q}, \omega)$ is the polarization operator defined by the phonon-electron interaction. We shall not discuss here the details of nonadiabatic effects in the normal state, but shall concentrate on measurements of the spectral density of phonons for $q = 0$ precisely in the transition to the superconducting state. The corresponding calculations of the polarization operator $\Pi_v(\omega)$ were carried out for both isotropic s-pairing [135] and anisotropic d-pairing [136, 137]. The expression for the function $\text{Im } \Pi_v(\omega)$ in the BCS model can be written in the form [136, 137]

$$\text{Im } \Pi_v(\omega) = \frac{-\pi N(\varepsilon_F)}{\omega} \left\langle \frac{|g_{\mathbf{k}}^v|^2 |\Delta(\mathbf{k})|^2 \theta(\omega^2 - [2\Delta(\mathbf{k})]^2)}{\sqrt{\omega^2 - [2\Delta(\mathbf{k})]^2}} \right\rangle \tanh \frac{\omega}{4T}, \quad (87)$$

where $g_{\mathbf{k}}^v$ is the EPI matrix element and the brackets imply averaging over the Fermi surface. In the case of isotropic s-pairing $\Delta(\mathbf{k})$ is a constant, and neglecting the dependence of $g_{\mathbf{k}}^v$ on \mathbf{k} we have

$$\text{Im } \Pi_v(\omega) = -\frac{\pi \lambda_v}{\omega} \frac{\Delta^2 \theta(\omega^2 - 4\Delta^2)}{\sqrt{\omega^2 - 4\Delta^2}} \tanh \frac{\omega}{2T}, \quad (88)$$

from which it is seen that phonons of energy $\omega < 2\Delta$ give

$$\text{Im } \Pi_v(\omega) = 0 \quad (89)$$

and damping is therefore absent. For phonons with $\omega > 2\Delta$, damping will on the contrary increase as the phonon energy approaches the value 2Δ . Using the Kramers–Kronig relation, one can calculate $\text{Re } \Pi_v(\omega)$ and determine the change of the phonon frequency from the relation

$$\omega_v^2 - \omega_0^2 - 2\omega_0 \text{Re } \Pi_v(\omega) = 0. \quad (90)$$

Phonons with $\omega < 2\Delta$ were shown [135] to become softer ($\omega_v < \omega_0$) and phonons with $\omega > 2\Delta$ to become harder

($\omega_v > \omega_0$) in transition to the superconducting state. The amplitude of these changes is completely determined by the coupling constant λ_v between a given mode and electrons. The behavior of a phonon of energy $\omega = 333 \text{ cm}^{-1}$ was explained in [135] in the framework of this approach on the assumption of s-pairing.

The situation is much more complicated in the case of d-pairing. The dependence of both the energy gap $\Delta(\mathbf{k})$ and the EPI matrix element $g_{\mathbf{k}}$ on the position of the vector \mathbf{k} on the Fermi surface becomes significant because of the averaging in formula (87) for $\text{Im } \Pi_v(\omega)$ over the Fermi surface. As shown in [137], the change of the function $\text{Im } \Pi_v(\omega)$ which describes the width of the phonon line is larger for phonons possessing the same symmetry as the energy gap $\Delta(\mathbf{k})$. The shift of the phonon frequencies changes accordingly. Thus, the change of phonons of different symmetries in the compound YBCO was described [137]. Nevertheless, the situation with the temperature dependence of the shift of phonon frequencies and their widths in HTSC systems remains not quite clear [138] and necessitates a consideration of anisotropic pairing with strong coupling. It is important that all these observations undoubtedly demonstrate the involvement of EPI in the superconducting pairing.

Further evidence in favor of the manifestation of EPI in the properties of the superconducting state follows from the analysis of the tunnel spectra of HTSC systems. As noted in the preceding section, the Eliashberg spectral function $\alpha^2(\omega)F(\omega)$ in the case of isotropic s-pairing can be obtained from the solution of the inverse problem for the Eliashberg equations (42), (43) with the known function $\Delta(\omega)$ reconstructed from measured tunnel characteristics of an SIN (superconductor–insulator–normal metal) junction. In this case, the derivative of the current I with respect to the voltage V is equal to

$$\frac{\partial I(V)}{\partial V} \sim N(V) \sim \text{Re} \left[\frac{V}{\sqrt{V^2 - \Delta^2(V)}} \right]. \quad (91)$$

There exist a large number of measurements of tunnel characteristics of HTSC systems, including measurements on standard flat SIN junctions [139, 140] and on so-called break junctions [141–143] in which a crystal break results in a tunnel junction. In these papers it was emphasized that the tunnel characteristics obtained in them differ little in form from those of typical s-superconductors. Moreover, they resemble the usual tunnel characteristics even more than we observe, for example, in the so-called electron-doped system $\text{Nd}_{2-x}\text{Ce}_x\text{CuO}_4$ [144] which in all other properties is certainly close to superconductors with the usual electron–phonon mechanism of pairing [31]. In papers [139–144] the tunnel characteristics were processed in the standard way for s-pairing, and the EPI spectral density shown in Fig. 18 was obtained. The same figure presents the density of phonon states obtained using neutron scattering [98] for comparison. As we can see, these curves agree rather well. It should however be emphasized that there exist a large number of other experiments on the tunnel characteristics of HTSC systems, including those performed using scanning tunnel electron microscopy [145, 146], in which the observed shapes of the $I(V)$ and $\partial I(V)/\partial V$ curves were so diverse that it is now extremely difficult to arrive at a definite conclusion about the role of EPI in HTSC systems from the study of tunnel characteristics only.

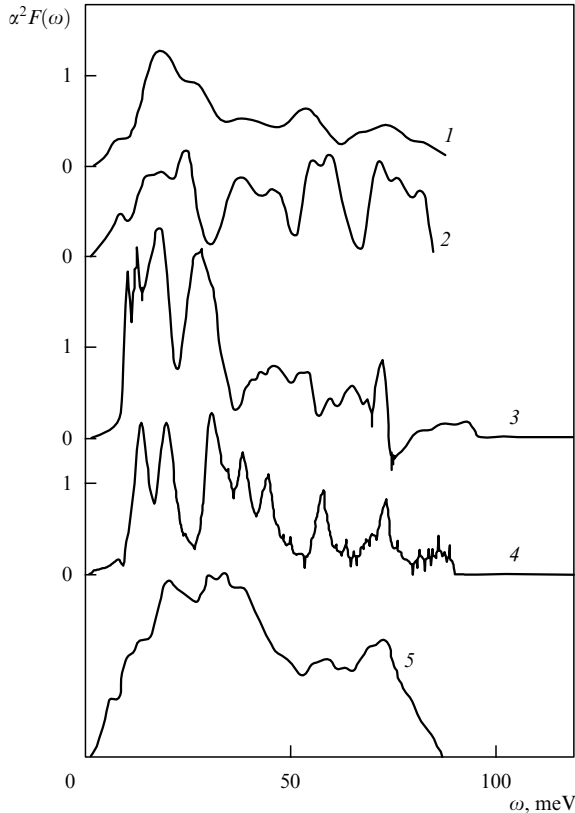


Figure 18. The function $|\partial^2 I / \partial V^2| \sim \alpha^2(\omega)F(\omega)$ obtained from tunnel experiments for HTSC systems. Figures 1, 2, 3, 4 mark the data of papers [141], [142], [140], and [139], respectively; 5 is the generalized density of phonon states measured in [98].

The existence of strong EPI in the superconducting state of HTSC systems was also confirmed by the recent observation [147] of a structure inside a superconducting gap in the tunnel characteristics of Josephson junctions with the current flowing perpendicularly to the CuO plane. The voltages for which these structures appeared correspond exactly to optical phonon energies.

In paper [148] it was shown that such a phenomenon is due to the interaction of Josephson current with phonons, more precisely, to the radiation of phonons upon electron tunneling through a junction, in the same manner as so-called Shapiro steps occur in conventional superconductors upon the interaction of Josephson current with electromagnetic radiation [149].

Concluding this discussion of experimental evidence that EPI also exists in the superconducting state of HTSC systems, we should mention the isotope effect. In single-component systems with electron–phonon interaction the value of the isotope effect $\alpha = d \ln T_c / d \ln M$ (where M is the isotope mass) is 1/2. It is a known fact [150] that in optimally doped systems the isotope effect, i.e. the dependence of T_c on the isotope mass, is practically equal to zero. This effect is nevertheless existent in a number of underdoped systems and its value reaches $\alpha_0 \approx 0.3$ for oxygen.

We should immediately point out that in spite of a large body of evidence in favor of the existence of strong EPI in HTSC systems, the standard approach to superconductivity based on the Eliashberg equations (42), (43) with isotropic pairing fails to explain the greater part of the superconducting

properties of such systems especially at low temperatures. This is apparent, for example, from Fig. 19 which reproduces the reflection coefficient for YBCO films from our paper [99]. The low temperature behavior of the calculated reflection coefficient differs substantially from that observed experimentally for both low ($\omega < 2\Delta$) and high ($\omega > 2\Delta$) energies. For the normal state, on the contrary, these two values coincide with very good accuracy (see Fig. 19). For low ω , the theoretical curve demonstrates a gap in the excitation spectrum with a ratio $2\Delta/T_c = 4.6$, whereas the experimental curves do not show this gap certainly. For high energies ($\omega > 2\Delta$), the calculated function $R(\omega)$ exhibits oscillations, typical of superconductors with s-pairing and a strong EPI, near the reflection coefficient at $T = T_c$ up to $\omega = 2000 \text{ cm}^{-1}$. We may state that the standard approach in the EPI framework cannot explain the two most characteristic properties of superconductivity in HTSC systems. These are, first, the strong anisotropy of the energy gap and, second, the high values of the ratio $2\Delta/T_c \sim 5-7$, which are even very high in $\text{La}_{2-x}\text{Sr}_x\text{CuO}_4$, where $2\Delta/T_c \approx 9$ [151], and in $\text{Bi}_2\text{Sr}_{2-x}\text{La}_x\text{CuO}_6$, where $2\Delta/T_c \approx 12$ [152]. It was also established [153] that in HTSC systems, not only the superconducting gap, but also the properties of the normal state are strongly anisotropic even in the CuO plane. Angle-resolved photoemission measurements revealed the absence of a well pronounced quasi-particle peak on the momentum axis $\mathbf{k} = (0, k_x)$ near the Fermi surface. In the superconducting state, a maximum of the energy gap $\Delta_{\mathbf{k}}$ appears on the same axis. Accordingly, a well pronounced quasi-particle peak exists in the normal state on the axis $k_x = k_y$, where $\Delta_{\mathbf{k}}$ vanishes. It is known [153] that in photoemission experiments one measures, to the simplest approximation, the spectral density of the one-particle Green function, i.e., the quantity

$$A(\mathbf{k}, \omega) = \frac{1}{\pi} \frac{\text{Im } \Sigma(\mathbf{k}, \omega)}{[\omega - \varepsilon_{\mathbf{k}} - \text{Re } \Sigma(\mathbf{k}, \omega)]^2 + [\text{Im } \Sigma(\mathbf{k}, \omega)]^2}. \quad (92)$$

Without going into the detail of possible explanations [118, 119] of the observed phenomenon, which are largely based on the effects of spin-fluctuation interactions, we note that for the indicated values of momentum \mathbf{k} , i.e. on the axis $(0, \pi)$, the quantities $\text{Re } \Sigma(\mathbf{k}_F, \omega)$ and $\text{Im } \Sigma(\mathbf{k}_F, \omega)$ reach their maximum values. Since both these quantities are at least

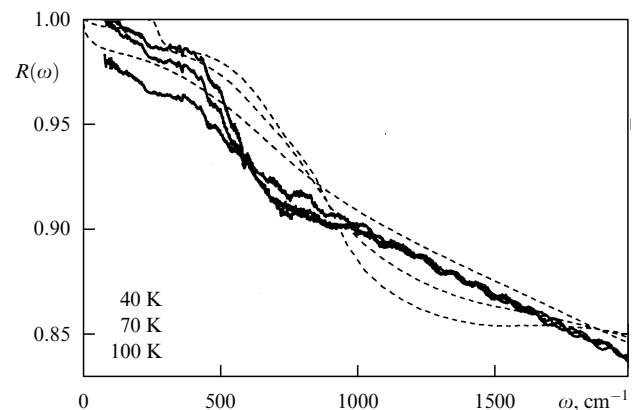


Figure 19. Measured (solid lines) and calculated (dashed lines) reflection coefficients for YBCO films at temperatures above and below T_c .

proportional to the interaction constant $\lambda_{\mathbf{k}}$, it follows in turn that this interaction is strongly anisotropic.

The corresponding anisotropic interaction exists in systems with strong antiferromagnetic spin fluctuations. This interaction can be written in the form [154]

$$V_{\text{eff}} \sim \frac{3}{2} U^2 \chi(\mathbf{k}' - \mathbf{k}), \quad (93)$$

where U is the electron repulsion on the Cu ion and $\chi(\mathbf{k}' - \mathbf{k})$ is the magnetic susceptibility. In the case of antiferromagnetic fluctuations, the function $\chi(\mathbf{k}' - \mathbf{k})$ has a sharp peak on the wave vector $\mathbf{k}' - \mathbf{k} = (\pi, \pi)$. The effective interaction $V_{\text{eff}}(\mathbf{q})$ is repulsive for all \mathbf{q} , and it is therefore easiest to understand the reason for the appearance of superconductivity with d-pairing under this interaction by considering the interaction among electrons (holes) in real space

$$V(\mathbf{R}) = \frac{1}{N} \sum_{\mathbf{q}} \exp(i\mathbf{q}\mathbf{R}) V_{\text{eff}}(\mathbf{q}). \quad (94)$$

The results of calculation of this function for the two-dimensional Hubbard model show [154] that the interaction of two electrons (holes) on a copper ion is very strong and repulsive. However, the interaction of electrons on the copper ion with electrons on the nearest neighboring oxygen ions is attractive. Such an interaction has an attractive d-harmonic and, according to the general ideas of pairing in various harmonics, a superconducting state with d-pairing may arise.

The objections we expressed in the preceding section to the possibility of explaining the relaxation processes in HTSC systems do not refer directly to the problem of the existence of superconducting d-pairing caused by antiferromagnetic spin fluctuations. The solution of the standard BCS equation in the d-channel leads to an expression for T_c :

$$T_c \simeq \omega_c \exp\left(-\frac{1}{\lambda}\right), \quad (95)$$

where ω_c is the characteristic energy of spin fluctuations and λ is the total coupling constant. Assuming ω_c to have the same order of magnitude as in the antiferromagnetic state of underdoped HTSC systems, i.e. $\omega_c \approx 0.4$ eV and $\lambda \sim 0.4-0.6$, one can readily obtain the resulting value $T_c \sim 50-80$ K. Calculations for the two-dimensional Hubbard model [155, 156] with allowance for vertex corrections in the interaction, which are necessary for the laws of conservation of current and charge to be obeyed, showed the possibility of reaching $T_c \sim 100$ K and the ratio $2\Delta/T_c \sim 8-10$. However, the interaction parameters set in these calculations seem to be rather far from realistic and strongly overestimate the ratio of the Hubbard repulsion U to the allowed band width W . In particular, the calculations [157] which made use of the magnetic susceptibility $\chi(\mathbf{q})$ taken from the neutron scattering measurements yield substantially lower T_c values.

A rather important circumstance, not to be forgotten in a consideration of any nonphonon anisotropic mechanism of superconductivity, is the strong EPI in HTSC systems, which in our opinion was convincingly demonstrated above. The effect of this interaction on anisotropic superconductivity can be easily understood from the example of the following simple model. Suppose a system possesses a mechanism inducing superconductivity in the d-channel and an isotropic EPI. The corresponding equations for the temperature $T = T_c$ can be

written in the form

$$Z(\omega) \Delta_{\mathbf{k}}(\omega) = \sum_{\mathbf{k}'} \int_0^{\omega_0} \frac{d\omega'}{\omega'} V_{\mathbf{k}\mathbf{k}'} \Delta_{\mathbf{k}'}(\omega) \tanh \frac{\epsilon_{\mathbf{k}'}}{2T_c}. \quad (96)$$

For the function $Z(\omega)$ one can write expression (43) from the preceding section. For our purpose it suffices that we restrict ourselves to allowing for the imaginary part of the function $Z(\omega)$, writing it as

$$Z = 1 + \frac{i}{\tau}. \quad (97)$$

Let us represent the interaction $V_{\mathbf{k}\mathbf{k}'}$ as

$$V_{\mathbf{k}\mathbf{k}'} = 2V \cos 2\varphi \cos 2\varphi', \quad (98)$$

where φ is the angle determining the position of the momentum \mathbf{k} on the Fermi surface, and, accordingly, $\Delta_{\mathbf{k}}(\omega)$ as

$$\Delta_{\mathbf{k}}(\omega) = \Delta(\omega) \sqrt{2} \cos 2\varphi. \quad (99)$$

Then we can readily solve equation (96) and obtain the expression for T_c [157]

$$\ln \frac{T_c}{T_c^0} = \Psi\left(\frac{1}{2}\right) - \Psi\left(1 + \frac{1}{2\pi T_c \tau}\right), \quad (100)$$

which is well-known from the theory of anisotropic superconductors with impurity scattering. In this expression T_c^0 is the critical transition temperature in the absence of EPI and $\Psi(x)$ is the usual digamma-function. This expression implies that the isotropic EPI acts on the critical temperature of a d-pairing superconductor as ordinary impurity scattering. It is of importance here that in HTSC systems this is a very strong scattering because

$$\frac{1}{\tau} = 2\pi\lambda T, \quad (101)$$

which is responsible for an appreciable lowering of T_c compared to T_c^0 . Roughly speaking, relations (100) and (101) imply

$$T_c \sim T_c^0 \exp(-\lambda), \quad (102)$$

where, according to the above discussion, λ is of the order of 2. This means that for obtaining experimental values $T_c \sim 100$ K a mechanism of anisotropic superconductivity must exist which by itself would give T_c values equal to $T_c^0 \sim 600-700$ K. Clearly, the existence of such mechanisms in nature is absolutely unrealistic.

Since the experimental discovery of HTSC cuprates, numerous attempts have been made to explain this phenomenon in the framework of the ordinary EPI (see reviews [30, 31, 158]). Such attempts are fully justified because, as we have already mentioned, the EPI spectral density taken from the analysis of the normal state relaxation processes may provide T_c values of the order of 100 K for isotropic pairing. These explanations are somewhat complicated by the recently established fact of the strong anisotropy of the energy gap in the majority of HTSC systems. However, a large number of studies have recently appeared (see papers [159-164] and references therein) reporting fairly successful attempts to reconcile the strong EPI with the strong anisotropy of the

energy gap. The main idea of all these papers is fairly simple. Suppose that electrons interact strongly only with phonons with small wave vectors $q < q_c$, where q_c satisfies the condition

$$q_c < k_F, K. \quad (103)$$

Here K is the reciprocal lattice vector. Suppose also that in the case of long-wave phonons the total coupling constant is sufficiently large, $\lambda \sim 2$, and may provide a T_c of the order of 60–100 K for isotropic pairing. The situation with the energy gap in this case can schematically be presented as follows. On a Fermi surface, isolated regions occur in which electrons interact strongly to one another owing to the coupling with long-wave phonons, while the interaction between the regions is weak because of the ineffectiveness of phonons with $q > q_c$. The sign of the order parameter in each of the regions is not defined because all the thermodynamic quantities depend, in fact, on the squared order parameter $|\Delta_{\mathbf{k}}|^2$. Thus, when an isotropic EPI alone is taken into account, degeneracy occurs with respect to the signs of the order parameter $\Delta_{\mathbf{k}}$ in different regions. Additional account of the Coulomb repulsion due to either spin fluctuations or Hubbard interaction of two holes on a copper ion lifts the degeneracy, and the d-component of the order parameter emerges over the entire Fermi surface. Since an attractive EPI is absent for large wave vectors connecting regions with opposite $\Delta_{\mathbf{k}}$ signs, the EPI does not have a destructive effect upon d-pairing.

There exist two serious problems associated with the above-discussed mechanism of the appearance of d-anisotropic superconductivity in the framework of the EPI model. The first problem is establishing the reason why electrons interact effectively with long-wave phonons only. The second problem is localization of isolated superconducting regions on the Fermi surface. A whole number of mechanisms have been proposed to solve the first problem. One of them [160–163] is related to the weakness of the Coulomb screening in quasi-two-dimensional systems with a high ionicity. The effective electron–electron interaction due to phonon exchange can roughly be presented in the form [160, 161]

$$V_{\text{eff}}(\mathbf{q}) = \sum_{\lambda} g_{\lambda}^2 \left(\frac{\kappa^2}{q^2 + \kappa^2} \right)^2 \frac{\omega_{\lambda}^2(\mathbf{q})}{(\varepsilon - \varepsilon')^2 - \omega_{\lambda}^2(\mathbf{q})}. \quad (104)$$

Here κ is the inverse radius of Debye screening whose value is assumed to be small

$$\kappa < k_F, K. \quad (105)$$

Formula (104) shows that because of the weak screening, i.e. fulfillment of inequality (105), the effective interaction exists only for long-wave phonons whose wave vectors q satisfy inequality (103).

Another possible mechanism of effective interactions with long-wave phonons was proposed in papers [164–166] (see also review [31]) and was associated with renormalization of the EPI matrix element through the exchange-correlation effects. This can likewise lead to the small matrix element for large transferred momenta.

The second of the above-mentioned problems, i.e. localization of superconducting regions on the Fermi surface, should also be solved. In the case of an isotropic EPI the centers of isolated superconducting regions can be located at any point of the Fermi surface, because in the normal state the electron–phonon coupling constant $\lambda_{\mathbf{k}}$ is the same over the

entire Fermi surface. The introduction of an additional anisotropic Coulomb repulsion can of course stabilize this situation in the superconducting state. However, the experimental data [153] indicate that there is a sufficiently strong anisotropy of the EPI constant in the normal state as well. To explain this fact, one can use the idea, developed in particular by Abrikosov [160, 161], of the existence of the extended Van Hove singularity in the spectra of HTSC systems. The essence of this phenomenon is that the energy spectra of electrons $\varepsilon(k_x, k_y)$ involve regions where $\varepsilon(k_x, k_y)$ does not depend on one of the components of momentum, and so the spectrum becomes quasi-one-dimensional. This leads in turn to a singularity (of the type $(\varepsilon - \varepsilon_0)^{-1/2}$, where ε_0 is the distance from the Fermi energy to the Van Hove singularity) in the density of electron states in the particular spectral region. There exists both experimental [153] and theoretical [167, 168] evidence supporting the presence of Van Hove singularities in HTSC systems, the singularities themselves lying on the axes $(0, \pi)$ and $(\pi, 0)$, i.e., precisely where the maxima of the energy gap and of the electron–phonon coupling constant in the normal state are located. The calculations carried out in papers [160, 161] thus allow the solution (with account of Van Hove singularity) of the problem of localization of superconducting regions and anisotropy of the EPI constant.

Not in the least depreciating the important role of Van Hove singularities or the predominant role of interaction with long-wave phonons, we shall only emphasize that many of the above-mentioned features of HTSC systems, such as the sharp anisotropy of relaxation and superconducting pairing, can in principle be explained in terms of EPI without involving any specific characteristics of the electron spectrum or scattering processes. We have already mentioned the *ab initio* calculations of EPI in YBCO [125] and CaCuO₂ [126] where EPI in HTSC cuprates was shown to be extremely anisotropic. In particular, the authors of [126] calculated the momentum-dependent EPI constant in different channels using the standard expression

$$\lambda_L(\mathbf{q}) \sim \sum_{\mathbf{k}, \nu} Y_L(\mathbf{k} + \mathbf{q}) |g_{\mathbf{q}\nu}^{\mathbf{k}}|^2 Y_L(\mathbf{k}) \delta(\varepsilon_{\mathbf{k}+\mathbf{q}}) \delta(\varepsilon_{\mathbf{k}}), \quad (106)$$

where $Y_L(\mathbf{k} + \mathbf{q})$ are the spherical harmonics. Here the component with $L = 0$ corresponds to a spherically symmetric EPI and the one with $L = 2$ — to the d-component of the EPI. It was shown [126] that in the compound CaCuO₂ the EPI constants in s- and d-channels are of the same order of magnitude, $\lambda_s \simeq \lambda_d$. It should however be noted that the absolute values of the constants λ_s and λ_d in CaCuO₂ turned out to be sufficiently small (~ 0.3), and they cannot explain the high $T_c \sim 90$ K observed in this compound. In contrast to this, the coupling constant $\lambda(\mathbf{q})$ in YBCO is shown in [125] to be strongly anisotropic and sufficiently large, $\lambda \sim 2$. As concerns the results for CaCuO₂ [126], one should bear in mind the uncertainty in the definition of the actual crystal structure of this compound [169] because not the compound CaCuO₂ itself, but a doped compound of the type $(\text{Ca}_{1-x}\text{Sr}_x)_{1-y}\text{CuO}_2$, where $x \approx 0.7$ and $y \approx 0.1$, is superconducting. The electronic structure of HTSC systems and the interaction of electrons in them depend very strongly on their crystal structure. The most vivid confirmation of this fact may be the disappearance of superconductivity in the $\text{La}_{2-x}\text{Ba}_x\text{CuO}_4$ system for barium concentrations $x \approx 0.125$ [170]. Moreover, for these Ba concentrations the antiferromagnetic ordering [171] returns. The change of the crystal structure actually observed in this case is very small [170, 171]

and is in fact reduced to a change of the axis of rotational displacement of octahedrons formed by oxygen ions surrounding the copper ion.

It is noteworthy that the hypothesis of the possible appearance of EPI-induced superconductivity in channels other than the isotropic s-pairing is not at all new. The possibility of p-pairing of electrons in alkali metals [172, 173] due precisely to EPI was discussed long before the discovery of HTSC cuprates. The EPI constants in alkali metals in the s-channel are notably smaller than in many other metals, $\lambda_s \approx 0.2$. The Coulomb pseudopotential in alkali metals has about the same order of magnitude, $\mu^* \approx 0.2$, which owing to the low electron density is somewhat larger than in many other metals where $\mu^* \approx 0.13$. Thus, according to the standard BCS expression for T_c

$$T_c \sim \omega_{\text{ph}} \exp\left(-\frac{1}{\lambda - \mu^*}\right) \quad (107)$$

superconductivity in the s-channel is either absent completely ($\lambda \lesssim \mu^*$) or the T_c value is exponentially small ($\lambda \gtrsim \mu^*$). The idea of possible existence of superconductivity in the p-channel in alkali metals rests on the following arguments. First, in anisotropic pairing the Coulomb isotropic repulsion exerts no influence on T_c^p which in this case can be written as

$$T_c^p \sim \omega_{\text{ph}} \exp\left(-\frac{1}{\lambda_p}\right). \quad (108)$$

Second, if the coupling constant λ_p satisfies the inequality

$$\lambda_p \geq |\lambda - \mu^*|, \quad (109)$$

superconductivity will occur in precisely the p-channel. The estimates of the quantity λ_p obtained in [172, 173] are rather contradictory, and experimentally superconductivity is not observed in alkali metals to very low temperatures. This means that λ_p in alkali metals hardly satisfies inequality (109).

A small value of the constant λ_p and, therefore, of the EPI anisotropy in alkali metals is not very surprising inasmuch as acoustic phonons alone exist in them, and all the interactions are strongly screened because the Thomas–Fermi screening length is small. The situation is radically different in HTSC systems containing a large number of optical phonons and exhibiting weak screening at least in the direction perpendicular to the CuO planes. In this respect, of considerable interest is the calculation [174, 175] of the interaction among electrons and the B_{1g} phonon. When the momentum is $q = 0$, such a phonon is characterized by the motion of oxygen ions, positioned in the CuO plane, away from this plane. Two of them, located on opposite sides of the copper ion, move upwards and the other two — downwards. With allowance for hybridization of only d wave functions of copper and p functions of oxygen, the following expression for the EPI matrix element $g_{B_{1g}}(\mathbf{k}, 0)$ was obtained [175]

$$g_{B_{1g}}(\mathbf{k}, q = 0) = g_{B_{1g}} \Phi_{B_{1g}}(\mathbf{k}), \quad (110)$$

where

$$\Phi_{B_{1g}}(\mathbf{k}) = \cos k_x - \cos k_y, \quad (111)$$

which is exactly the EPI d-component.

An important fact noted in papers [174, 175] is that

$$g_{B_{1g}} \equiv 0, \quad (112)$$

if the CuO plane is the mirror plane perpendicular to the c axis. This is precisely the case with the compound La_2CuO_4 , whereas in $\text{YBa}_2\text{Cu}_3\text{O}_7$ this mirror symmetry is broken because of the diverse surrounding of the plane. This circumstance may to some extent be an indication of the possible reason for a low value of T_c in lanthanum compounds compared to yttrium ones.

When discussing EPI anisotropy we have up to now mainly given examples of the existence of the d-component in the EPI matrix element in HTSC systems. Among the variety of optical modes in HTSC systems the modes exist whose EPI matrix elements possess other kinds of symmetry, including the so-called generalized s-symmetry:

$$g \sim \cos k_x + \cos k_y. \quad (113)$$

The question of what symmetry is actually inherent in the order parameter (or in the energy gap) in HTSC systems remains disputable. There is not the slightest doubt that this order parameter, at least in optimally doped systems, is strongly anisotropic and its amplitude is equal (or close) to zero in some regions of the Fermi surface. This was convincingly demonstrated in experiments on angle-resolved photoemission and in measurements of thermodynamic characteristics of HTSC systems (for more details see review [176]). Such experiments cannot however answer the question of whether the order parameter reverses sign along the Fermi surface, i.e., whether it possesses d-symmetry and if this is a pure d-symmetry or there is an admixture of other symmetries, including the isotropic s-symmetry. The answer to this question can only be given by experiments sensitive to the phase of the order parameter. Such experiments involve investigations of the Josephson tunneling, i.e., the superconducting current through dielectric junctions between superconductors. An extensive discussion of this question is also given in review [176] and we shall not dwell on it here, but only mention the following fact. Some experiments of this type [177] point to a practically perfect d-symmetry of the order parameter, others [178] to a substantial admixture of s-symmetry, and there are such [179] that show the prevailing role of precisely s-symmetry. No consensus concerning this issue has yet been reached.

Concluding this section we would like to mention briefly some models, described in the literature on HTSC systems, in which the superconducting state may occur owing to ‘the peaceful co-existence’ of a strong EPI with Coulomb repulsion. Some of them have already been discussed above, and therefore we shall now concentrate on those not mentioned earlier. These are first of all models explicitly allowing the multi-band electronic spectrum of HTSC systems [180–182]. Allowing further for the attraction of electrons due to EPI in one band and the repulsion due to Coulomb interaction in another band, one can rather simply explain many experimental data at low temperatures, including different signs of the order parameter. Furthermore, as shown in papers [180, 182], hybridization of such bands may yield zeros of the order parameter and its sign reversal in certain regions of momentum space. This problem was rather thoroughly analyzed in [182], where it was shown that if the wave functions of electrons from different bands have different symmetries, then irrespective of the nature of electron–electron interaction the order parameter may be strongly anisotropic owing to anisotropy of the hybridization matrix element of the bands. We should also mention the

model, due to P Anderson [183], of high-temperature superconductivity based on the Josephson interlayer tunneling. The equations of superconductivity for this model can be written in the form [183–185]

$$\Delta(\mathbf{k}) = T_j(\mathbf{k}) \frac{\Delta(\mathbf{k})}{2E_{\mathbf{k}}} \tanh \frac{E_{\mathbf{k}}}{2T} + \sum_{\mathbf{k}'} V_{\mathbf{k}\mathbf{k}'} \frac{\Delta(\mathbf{k}')}{2E_{\mathbf{k}'}} \tanh \frac{E_{\mathbf{k}'}}{2T}, \quad (114)$$

where

$$E_{\mathbf{k}} = \sqrt{\varepsilon_{\mathbf{k}} + [\Delta(\mathbf{k})]^2}. \quad (115)$$

One can readily derive these equations considering two CuO layers with the potential $V_{\mathbf{k}\mathbf{k}'}$ of electron–electron interaction in either layer and the interlayer interaction described by the Josephson tunnel Hamiltonian

$$H_j = \sum_{\mathbf{k}} T_j(\mathbf{k}) (c_{\mathbf{k}\uparrow}^+ c_{-\mathbf{k}\downarrow}^+ c_{-\mathbf{k}\uparrow} c_{\mathbf{k}\downarrow} + \text{H.c.}). \quad (116)$$

The equation specifying T_c in this model has the form

$$\Delta(\mathbf{k}) = \left[1 - \frac{T_j(\mathbf{k}) \tanh(\varepsilon_{\mathbf{k}}/2T_c)}{2\varepsilon_{\mathbf{k}}} \right]^{-1} \sum_{\mathbf{k}'} V_{\mathbf{k}\mathbf{k}'} \frac{\Delta(\mathbf{k}')}{2\varepsilon_{\mathbf{k}'}} \tanh \frac{\varepsilon_{\mathbf{k}'}}{2T_c}. \quad (117)$$

According to the ideas of Anderson himself [183], the intralayer interaction $V_{\mathbf{k}\mathbf{k}'}$ and its origin are of no importance for the existence of superconductivity as T_c is specified by the condition

$$T_c = \frac{[T_j(\mathbf{k}_F)]_{\max}}{4}. \quad (118)$$

This theory in its literal form encounters difficulties in the description of so-called single-layer systems and contradicts the experimental data on the magnetic field penetration depth [186, 187]. Nevertheless, an account of Josephson interplanar tunneling may be fairly significant for some HTSC systems, where it may appreciably increase the value of T_c in comparison with T_c determined only by the intraplanar interaction $V_{\mathbf{k}\mathbf{k}'}$. Moreover, in view of the fact that the matrix element of tunneling $T_j(\mathbf{k})$ is sharply anisotropic [185]

$$T_j(\mathbf{k}) \sim (\cos k_x - \cos k_y)^2, \quad (119)$$

such an account may strengthen precisely the anisotropic channel of pairing.

There also exist many other possibilities of the enhancement of superconducting pairing through a combined influence of attractive EPI and Coulomb repulsion, but a comprehensive discussion of these oversteps the limits of our review.

5. Conclusion, or is there light at the end of the tunnel?

To begin, we shall formulate the results of the above discussions.

It was shown that superconducting cuprates differ very little from other ‘conventional’ metals from the point of view of their excitation spectra for sufficiently high and moderate energies. All these spectra can to a good accuracy be calculated within DFT. Even low-energy interband transitions for $\text{YBa}_2\text{Cu}_3\text{O}_7$ can be calculated, the energies of such

transitions and their intensities being perfectly described by experimental data.

We should also point out one circumstance, which was practically not discussed here, namely that DFT in cuprates demonstrates undoubted effectiveness in the field of its standard application, i.e., in calculations of such ground-state properties as specific volume, elastic moduli, and phonon frequencies [80].

We have also shown in the review that experimental data on optical spectra, transport phenomena, and angle-resolved photoemission convincingly demonstrate the presence of strong relaxation processes in the low-energy range in the normal state of HTSC systems. Over a wide energy range, the inverse lifetimes $1/\tau$ of electron excitations significantly exceed the values of the excitation energies themselves, and the behavior of their electron system differs substantially from the behavior of the system of a weakly interacting Fermi gas of quasi-particles. However such behavior is also observed in all other metals in the temperature range where, in fact, the normal state of cuprates exists, with the only difference being that the absolute $1/\tau$ values themselves are much higher in cuprates than in many metals.

On the basis of our earlier calculations we have shown here that the majority of peculiarities of the low-energy relaxation in HTSC systems can simply and consistently be explained in terms of the standard strong EPI. Furthermore, it has been demonstrated that neither the residual quasi-particle Landau-type interaction, nor the interaction with spin fluctuations can describe the relaxation processes in HTSC systems because they lead to $1/\tau$ values one or two orders of magnitude lower than are expected from experiment.

The solution of the Eliashberg equations with the EPI spectral density extracted from optical spectra shows that EPI may well provide the temperature $T_c \sim 100$ K.

However, EPI in itself can hardly guarantee the anisotropic d-pairing observed in cuprates, and therefore something else must exist that determines, together with EPI, the mechanism of superconductivity in HTSC systems. We have considered a whole number of models here allowing the description of the superconducting state of cuprates with account of EPI and Coulomb repulsion. It has also been noted that in these systems the EPI itself is strongly anisotropic with a large component of d-symmetry.

What has been said above does not at all mean that all the problems associated with the behavior of HTSC systems in both the normal and the superconducting state can be thought of as solved. There remain many questions, including the concrete mechanism of the combined effect of EPI and Coulomb repulsion on the electron pairing, to which we cannot now give clear and distinct answers. Also quite dubious is the nature of the linear dependence of electrical resistivity when it extends up to temperatures $T \sim 10$ K. Still more obscure is the origin of the quadratic dependence $\rho(T)$ in overdoped HTSC systems because all the available argumentation in the framework of the Landau Fermi-liquid theory is certainly flimsy.

Among the unsolved problems which we have not yet discussed, we can mention, for example, charge separation in underdoped systems and the appearance in them of a ‘pseudogap’ at temperatures greatly exceeding the superconducting transition temperature. Although of undoubted interest and importance for the understanding of the phenomena observed in HTSC systems, all these problems have to be left beyond the scope of this review because, as the

well-known Russian aphorism says, “one cannot embrace the unembraceable”.

We shall now briefly discuss the question, put in the title of this section, of whether there is light at the end of the tunnel. Generally speaking, the answer to this question is entirely a matter of opinion. Some people believe that the light has never faded, while others think that no light is yet seen ahead. Much more important to the scientific community is the fact that the total number of tunnels in the HTSC problem now definitely exceeds all reasonable limits, and from within such tunnels one fails sometimes to see not only the light at the end, but even the very existence of other tunnels.

It is a pleasure for me to express in conclusion my deep gratitude to a large number of my colleagues and friends for numerous discussions and their help in the preparation of this review. In the first place I would like to mention V L Ginzburg, owing to the persistence and everyday care of whom the review was written. I am also thankful to O V Dolgov, A E Karakozov, O K Andersen, N Bontemps, R Combescot, M L Kulić, H J Kaufmann, D Rainer, and E K H Salje.

I thank the Russian Foundation for Basic Research (grant 99-02-16366), the governmental HTSC program, the Russian ‘Integration’ Foundation (grant A0075), ISTC (project N 207), as well as the Royal Society and CNRS.

References

- Ginzburg V L *Phys. Lett.* **13** 101 (1964)
- Little W A *Phys. Rev. A* **134** 1416 (1964)
- Bednorz J G, Müller K A *Z. Phys. B* **64** 189 (1986)
- Wu M K et al. *Phys. Rev. Lett.* **58** 908 (1987)
- Putilin S N et al. *Nature* (London) **362** 226 (1993)
- Chu C W et al. *Nature* (London) **365** 323 (1993)
- Problema Vysokotemperaturnoi Sverkhprovodimosti* (Eds V L Ginzburg, D A Kirzhnits) (M.: Nauka, 1977) [Translated into English: *High-Temperature Superconductivity* (Eds V L Ginzburg, D A Kirzhnits) (New York: Consultants Bureau, 1982)]
- Cohen M L, Anderson P W, in *Superconductivity in d- and f-Band Metals* (AIP Conf. Proc., Ed D H Douglass) (New York: AIP, 1972) p. 17
- Dolgov O V, Maksimov E G *Usp. Fiz. Nauk* **135** 441 (1981) [*Sov. Phys. Usp.* **24** 1019 (1981)]
- Pashitskiĭ E A *Fiz. Nizk. Temp.* **21** 995 (1995)
- Dolgov O V, Maksimov E G *Usp. Fiz. Nauk* **138** (1) 95 (1982) [*Sov. Phys. Usp.* **25** 688 (1982)]
- Anderson P W *The Theory of Superconductivity in the High-T_c Cuprates* (Princeton: Princeton Univ. Press, 1997)
- Kalmeyer V, Laughlin R B *Phys. Rev. Lett.* **59** 2095 (1987); Affleck I, Marston J B *Phys. Rev. B* **37** 3664 (1988)
- Anderson P W *Science* **235** 1136 (1987)
- Luttinger J M *J. Math. Phys.* **15** 609 (1963)
- Anderson P W, in *High-Temperature Superconductivity* (AIP Conf. Proc., Vol. 483, Eds S E Barnes et al.) (Woodbury, N.Y.: AIP, 1999) p. 3
- Spielman S et al. *Phys. Rev. Lett.* **65** 123 (1990)
- Gammel P L et al. *Phys. Rev. B* **41** 2593 (1990)
- Norman M R *J. Phys. Chem. Sol.* **54** 1165 (1993)
- Leggett A *Phys. World* **10** 51 (1997)
- Monien H, Pines D *Phys. Rev. B* **41** 6297 (1990)
- Mills A, Monien H *Phys. Rev. B* **45** 3059 (1992)
- Schrieffer J R, Wenx G, Zhang S C *Phys. Rev. B* **39** 11663 (1990)
- Kampf A, Schrieffer J R *Phys. Rev. B* **41** 6399 (1990)
- Ruvalds J *Supercon. Sci. Technol.* **9** 905 (1996)
- Kohn W, Luttinger J M *Phys. Rev. Lett.* **15** 524 (1965)
- Akhiezer A I, Pomeranchuk I L *Zh. Eksp. Teor. Fiz.* **36** 859 (1959) [*Sov. Phys. JETP* **9** 605 (1959)]
- Mineev V P *Usp. Fiz. Nauk* **139** 303 (1983) [*Sov. Phys. Usp.* **26** 160 (1983)]
- Fulde P, Keller J, Zwicknagl G, in *Solid State Physics* Vol. 41 (Eds H Ehrenreich, H Turnbull) (New York: Academic, 1986) p. 2
- Pashitskiĭ E A *Fiz. Nizk. Temp.* **21** 1091 (1995)
- Kulić M L *Phys. Rep.* (2000, in press)
- Kirzhnits D A *Usp. Fiz. Nauk* **119** 357 (1976) [*Sov. Phys. Usp.* **19** 530 (1976)]
- Dolgov O V, Kirzhnits D A, Maksimov E G *Rev. Mod. Phys.* **53** 81 (1981)
- Fasolino A, Parrinello M, Tosi M P *Phys. Lett. A* **66** 119 (1978)
- Kittel C *Quantum Theory of Solids* (New York: Wiley, 1963) [Translated into Russian (Moscow: Nauka, 1967)]
- Schofield A J *Contemp. Phys.* **40** 95 (1998)
- Allen P B *Comments Cond. Math. Phys.* **15** 327 (1992)
- Landau L D *Zh. Eksp. Teor. Fiz.* **30** 1058 (1956) [*Sov. Phys. JETP* **3** 920 (1957)]
- Bloch F *Z. Phys.* **52** 555 (1928)
- Gell-Mann M, Brueckner K A *Phys. Rev.* **106** 364 (1957)
- Silin V P *Zh. Eksp. Teor. Fiz.* **33** 495 (1957) [*Sov. Phys. JETP* **6** 389 (1958)]
- Lifshits I M, Azbel’ M Ya, Kaganov M I *Elektronnaya Teoriya Metallov* (Electron Theory of Metals) (Moscow: Nauka, 1971) [Translated into English (New York: Consultants Bureau, 1973)]
- Rainer D, in *Progress in Low Temperature Physics* Vol. X (Ed. D C Brewer) (Amsterdam: Elsevier, 1986) p. 371
- Eliashberg G M *Zh. Eksp. Teor. Fiz.* **41** 1241 (1961) [*Sov. Phys. JETP* **14** 970 (1962)]
- Keldysh L V *Zh. Eksp. Teor. Fiz.* **47** 1515 (1964) [*Sov. Phys. JETP* **20** 1018 (1965)]
- S Lundqvist, N H March (Eds) *Theory of the Inhomogeneous Electron Gas* (New York: Plenum, 1983) [Translated into Russian: D A Kirzhnits, E G Maksimov (Eds) (Moscow: Mir, 1987)]
- Migdal A B *Zh. Eksp. Teor. Fiz.* **34** 1438 (1958) [*Sov. Phys. JETP* **7** 996 (1958)]
- Eliashberg G M *Zh. Eksp. Teor. Fiz.* **38** 966; **39** 1437 (1960) [*Sov. Phys. JETP* **11** 696 (1960); **12** 1000 (1961)]
- Holstein T D *Ann. Phys. (N.Y.)* **29** 410 (1964)
- Allen P B, Mitrovich B, in *Solid State Physics* Vol. 37 (Eds H Ehrenreich, F Seitz, D Turnbull) (New York: Academic, 1982) p. 1
- Maksimov E G, Savrasov D Yu, Savrasov S Yu *Usp. Fiz. Nauk* **167** 353 (1997) [*Phys. Usp.* **40** 337 (1997)]
- Allen P B *Phys. Rev. B* **3** 305 (1971)
- Kaufmann H J, Maksimov E G, Salje E K H *J. Supercond.* **11** 755 (1998)
- Modine F A et al. *Phys. Rev. B* **40** 9558 (1989)
- Beaulac T P, Allen P B, Pinski F J *Phys. Rev. B* **26** 1549 (1982)
- McMillan W L, Rowell J M, in *Superconductivity* Vol. 1 (Ed. R D Parks) (New York: M. Dekker, 1969) p. 561
- Svistunov V M, Belogolovskii M A, Khachapurov A I *Usp. Fiz. Nauk* **163** 61 (1993) [*Phys. Usp.* **36** 65 (1993)]
- Motulevich G P *Usp. Fiz. Nauk* **97** 211 (1969) [*Sov. Phys. Usp.* **12** 74 (1969)]
- Farnworth B, Timusk T *Phys. Rev. B* **14** 5119 (1976)
- Klein B M, Pickett W F, in *Superconductivity in d- and f- Band Metals* (Eds W Buckel, W Weber) (Karlsruhe: Kernforschungszentrum, 1982) p. 447
- Savrasov S Yu, Maksimov E G *Usp. Fiz. Nauk* **165** 773 (1995) [*Phys. Usp.* **38** 737 (1995)]
- Kohn W, Sham L J *Phys. Rev. A* **140** 1133 (1965)
- Jones R O, Gunnarsson O *Rev. Mod. Phys.* **61** 689 (1989)
- Schönhammer K, Gunnarsson O *Phys. Rev. B* **37** 3128 (1988)
- Luttinger J M *Phys. Rev.* **119** 1153 (1960)
- Eliashberg G M, Von der Linden W *Pis'ma Z. Eksp. Teor. Fiz.* **59** 413 (1994) [*JETP Lett.* **59** 441 (1994)]
- J. Phys. Chem. Solids* **54** (11/12) (1993)
- Mazin I I et al. *Zh. Eksp. Teor. Fiz.* **90** 1092 (1986) [*Sov. Phys. JETP* **63** 637 (1986)]
- Maksimov E G et al. *J. Phys. F* **18** 833 (1988)
- Mazin I I et al. *Tr. Fiz. Inst. Akad. Nauk SSSR* **190** 4 (1988) [Translated into English: *Metal Optics and Superconductivity* (New York: Nova Science, 1991)]
- Fehrenbach G-M *Phys. Rev. B* **59** 15085 (1999)
- Gross E K U, Dobson J F, Petersilka M, in *Density Functional Theory* (Ed. R F Nalivaitski) (Berlin: Springer, 1996) p. 71
- Uspenskiĭ Yu A, Kulatov E T, Khalilov S V *Zh. Eksp. Teor. Fiz.* **107** 1708 (1995) [*JETP* **80** 952 (1995)]

74. Savrasov S Yu, Savrasov D Yu *Phys. Rev. B* **46** 12181 (1992)
75. Savrasov S Yu, Savrasov D Yu, Andersen O K *Phys. Rev. Lett.* **72** 372 (1994)
76. Sternheimer R M *Phys. Rev. A* **96** 951 (1954)
77. Mahan G D *Many-Particle Physics* (New York: Plenum, 1981)
78. Yasuhare H, Onsaka Y *Int. J. Mod. Phys. B* **6** 3089 (1992)
79. Antonov V N et al. *Zh. Eksp. Teor. Fiz.* **95** 732 (1989) [*Sov. Phys. JETP* **68** 415 (1989)]
80. Pickett W E *Rev. Mod. Phys.* **61** 433 (1989)
81. Mazin I I et al. *Pis'ma Zh. Eksp. Teor. Fiz.* **47** 94 (1988) [*JETP Lett.* **47** 113 (1988)]
82. Maksimov E G et al. *Phys. Rev. Lett.* **63** 1880 (1989)
83. Rashkeev S N et al. *Zh. Eksp. Teor. Fiz.* **97** 1688 (1990) [*Sov. Phys. JETP* **70** 952 (1990)]
84. Chui S T, Kasowski R V, Hsu W Y *Phys. Rev. Lett.* **61** 885 (1988)
85. Chen H et al. *Phys. Rev. B* **43** 383 (1991)
86. Ushida S et al. *Phys. Rev. B* **43** 7942 (1991)
87. Tajima S et al. *J. Opt. Soc. Am.* **6** 475 (1989)
88. Rombers H et al. *Z. Phys. B.* **78** 367 (1980)
89. Balzarotti A et al. *Sol. State Commun.* **68** 381 (1988)
90. Nücker N et al., in *Studies of High Temperature Superconductors* Vol. 10 (Ed. A Narlikar) (New York: Nova Science, 1989) p. 132
91. Bucker B et al. *Phys. Rev. B* **45** 3026 (1992)
92. Petrov M P et al. *Pis'ma Zh. Eksp. Teor. Fiz.* **50** 25 (1989) [*JETP Lett.* **50** 29 (1989)]
93. Renk K F et al. *Physica C* **165** 1 (1996)
94. Schlesinger Z et al. *Phys. Rev. Lett.* **65** 801 (1990)
95. Schmitt-Rink S, Varma C M, Ruckenstein A E *Phys. Rev. Lett.* **60** 2793 (1988)
96. Shulga S V, Dolgov O V, Maksimov E G *Physica C* **178** 266 (1991)
97. Bozovich I *Phys. Rev. B* **42** 1969 (1990)
98. Pintschovis L, Reichardt W, in *Physical Properties of High-Temperature Superconductors* Vol. IV (Ed. D M Ginzberg) (Singapore: World Scientific, 1994) p. 295
99. Maksimov E G et al. *Solid State Commun.* **112** 449 (1999)
100. Kaminski A et al. *Phys. Rev. Lett.* **84** 1388 (2000)
101. Anderson P W *Phys. Rev. B* **55** 11785 (1997)
102. Romero D B et al. *Solid State Commun.* **82** 183 (1992)
103. Jehl G et al. *Europhys. Lett.* **16** 330 (1991)
104. Kaufmann H J, Ph D Thesis (Cambridge: Cambridge Univ., 1999)
105. Dolgov O V, Shulga S V *J. Supercond.* **8** 611 (1995)
106. Carbotte J P, Schaschinger E, Basov D N *Nature* (London) **401** 354 (1999)
107. Ginzburg V L, Maksimov E G *Physica C* **235–240** 193 (1994)
108. Fong H F et al. *Phys. Rev. B* **54** 6708 (1996)
109. Smith T J et al. *J. Supercond.* **12** 95 (1999)
110. Chuang Y -D et al. *Phys. Rev. Lett.* **83** 3717 (1999)
111. Zakharov A A et al. *Phys. Rev. B* **61** 115 (2000)
112. Fretwell H M et al. *Phys. Rev. Lett.* **84** 4449 (2000)
113. Borisenko S V et al. *Phys. Rev. Lett.* **84** 4453 (2000)
114. Fiory A T et al. *Physica C* **162–164** 1195 (1989)
115. Mackenzie A et al. *Physica C* **162–164** 1029 (1989)
116. Vedenev S I et al. *Phys. Rev. B* **51** 16380 (1995)
117. Gurzhi R N, Kopeliovich A I, Rutkevich S B *Adv. Phys.* **36** 221 (1987)
118. Stojkovic B P, Pines D *Phys. Rev. B* **55** 8576 (1997)
119. Ioffe L B, Millis A J *Phys. Rev. B* **58** 11631 (1998)
120. Jarlborg T *Solid State Commun.* **71** 669 (1989)
121. Cohen R E, Pickett W E, Krakauer H *Phys. Rev. Lett.* **64** 2575 (1990)
122. Zeyher R *Z. Phys. B* **80** 187 (1990)
123. Krakauer H, Pickett W E, Cohen R E *Phys. Rev. B* **47** 1002 (1993)
124. Mazin I I et al., in *Lattice Effects in High-T_c Superconductors* (Eds Y Bar-Yam et al.) (Singapore: World Scientific, 1992) p. 235
125. Zhao G L, Browne D A, Callaway J *Phys. Rev. B* **52** 16217 (1995)
126. Savrasov S Yu, Andersen O K *Phys. Rev. Lett.* **77** 4430 (1996)
127. Litvinchuk A P, Thomsen O, Cardona M, in *Physical Properties of High-Temperature Superconductors* Vol. IV (Ed. D M Ginzberg) (Singapore: World Scientific, 1994) p. 375
128. Thomsen C, in *Light Scattering in Solids* Vol. VI (Eds M Cardona, G Güntherodt) (Berlin: Springer, 1991) p. 285
129. Hadjev V G et al. *Phys. Rev. B* **58** 1043 (1998)
130. Engelsberg S, Schrieffer J R *Phys. Rev.* **131** 553 (1963)
131. Schuster H G *Solid State Commun.* **13** 1559 (1973)
132. Maksimov E G, Shulga S V *Solid State Commun.* **97** 553 (1936)
133. Karakozov A E, Maksimov E G *Zh. Eksp. Teor. Fiz.* **115** 1799 (1999) [*JETP* **88** 987 (1999)]
134. Ponosov Yu S et al. *Phys. Status Solidi B* **208** 257 (1998)
135. Zeyher R, Zwicky G *Z. Phys. B* **78** 175 (1990)
136. Nicol E J, Jiang C, Carbotte J P *Phys. Rev. B* **47** 8131 (1999)
137. Devereaux T P *Phys. Rev. B* **50** 10287 (1994)
138. Zhigadlo N N, Zhang M, Salje E K H *Supercond. Sci. Technol.* **10** 209 (1997)
139. Shimada D et al. *Phys. Rev. B* **51** 16495 (1995)
140. Miyakawa N et al. *J. Phys. Soc. Jpn.* **62** 2445 (1993)
141. Vedenev S I, Jensen A G M, Wyder P *Physica B* **218** 213 (1996)
142. Gonnelli R S, Asdente F, Andreone D *Phys. Rev. B* **49** 1486 (1994)
143. Aminov B A et al. *Physica C* **235–240** 1863 (1994)
144. Kashiwaya S et al. *Phys. Rev. B* **56** 13746 (1997)
145. Hasegawa T et al. *J. Supercond.* **8** 467 (1995)
146. Renner C, Fischer O *Phys. Rev. B* **51** 9208 (1995)
147. Ponomarev Ya G et al. *Solid State Commun.* **111** 513 (1999)
148. Maksimov E G, Arseyev P I, Maslova N S *Solid State Commun.* **111** 391 (1999)
149. Kulik I O *Pis'ma Zh. Eksp. Teor. Fiz.* **2** 134 (1965) [*JETP Lett.* **2** 82 (1965)]
150. Frank J F, in *Physical Properties of High-Temperature Superconductors* Vol. V (Ed. D M Ginzberg) (Singapore: World Scientific, 1994)
151. Ekino T et al. *Physica C* **263** 249 (1996)
152. Schmidt H et al., in *Proc. M²S Conf.* (Houston, 2000); *Physica C* (to be published)
153. Zhen Z-X, Dessau D S *Phys. Rep.* **253** 1 (1995)
154. Scalapino D J *Phys. Rep.* **251** 154 (1994)
155. Monthoux P, Scalapino D J *Phys. Rev. Lett.* **72** 1874 (1994)
156. Pao C-H, Bickers N E *Phys. Rev. Lett.* **72** 1870 (1994)
157. Radtke R J et al. *Phys. Rev. B* **48** 15957 (1993)
158. Ginzburg V L, Maksimov E G *Sverkhprov. Fiz., Khim., Tekh.* **5** 1543 (1992) [*Supercond. Phys. Chem. Technol.* **5** 1505 (1992)]
159. Maksimov E G *J. Supercond.* **8** 433 (1995)
160. Abrikosov A A *Physica C* **222** 191 (1994)
161. Abrikosov A A *Phys. Rev. B* **53** R8910 (1996)
162. Santi G et al. *J. Supercond.* **8** 405 (1995)
163. Peter M, Weger M, Pitaevskii L P *Ann. Phys.* (Berlin) **7** 174 (1998)
164. Dolgov O V et al. *Int. J. of Mod. Phys. B* **12** 3083 (1998)
165. Varelogiannis G *Physica C* **317–318** 238 (1999)
166. Grimaldi C, Pietronero L, Strässler S *Phys. Rev. B* **52** 10530 (1995)
167. Novikov D L, Freeman A J *Physica C* **216** 273 (1993)
168. Andersen O K et al. *Phys. Rev. B* **49** 4145 (1994)
169. Shaked H et al. *Phys. Rev. B* **51** 11784 (1995)
170. Moodenbauch A R et al. *Phys. Rev. B* **38** 4596 (1998)
171. Kumagai K et al. *J. Magn. Magn. Mat.* **76–77** 601 (1988)
172. Appel J, Heusenau H *Phys. Rev.* **188** 755 (1969)
173. Foulkes I F, Gyorffy B L *Phys. Rev. B* **15** 1335 (1977)
174. Barišić S, Batistić J *Europhys. Lett.* **8** 765 (1989)
175. Devereaux T P, Virosztek A, Zawadowski A *Phys. Rev. B* **51** 505 (1995)
176. Annett J F, Goldenfeld N, Leggett A J, in *Physical Properties of High-Temperature Superconductors* Vol. 5 (Ed. D M Ginzberg) (Singapore: World Scientific, 1995) p. 375
177. Tsuei C C et al. *Phys. Rev. Lett.* **73** 593 (1994)
178. Bhattacharya A et al. *Phys. Rev. Lett.* **82** 3132 (1999)
179. Li Q et al. *Phys. Rev. Lett.* **83** 4160 (1999)
180. Combescot R, Leyronas X *Phys. Rev. Lett.* **75** 3732 (1995)
181. Golubov A A et al. *Physica C* **235–240** 2383 (1994)
182. Arseyev P I, Fedorov M K, Volkov B A *Solid State Commun.* **100** 581 (1996)
183. Chakravarty S et al. *Science* **261** 337 (1993)
184. Sudbø A *J. Low Temp. Phys.* **97** 403 (1994)
185. Sardar M *Physica C* **298** 254 (1998)
186. Van der Marel D et al. *Physica C* **235–240** 1145 (1994)
187. Moler K A et al. *Science* **279** 1193 (1998)